Journal of Hydrology 577 (2019) 123936

Contents lists available at ScienceDirect

Journal of Hydrology

journal homepage: www.elsevier.com/locate/jhydrol

Research papers

# Coupling hydrodynamic, geochemical and isotopic approaches to evaluate oxbow connection degree to the main stream and to adjunct alluvial aquifer

M. Quenet[a,*], H. Celle-Jeanton[b], O. Voldoire[a], J. Albaric[b], F. Huneau[c,d], J.-L. Peiry[e], E. Allain[a], A. Garreau[a], A. Beauger[a]

[a] Université Clermont Auvergne, CNRS, GEOLAB, F-63000 Clermont-Ferrand, France
[b] Laboratoire Chrono-environnement – UMR 6249 CNRS-UFC, 16 Route de Gray, 25030 Besançon, France
[c] Université de Corse Pascal Paoli, Faculté des Sciences et Techniques, Département d'Hydrogéologie, Campus Grimaldi, BP 52, F-20250 Corte, France
[d] CNRS, UMR 6134, SPE, F-20250 Corte, France
[e] Unité Mixte Internationale 3189 «Environnement, Santé, Sociétés » – CNRS UMIESS, Université Cheikh Anta Diop, Faculté de Médecine, BP 5005, Dakar Fann, Senegal

ARTICLE INFO

This manuscript was handled by Huaming Guo, Editor-in-Chief, with the assistance of Seong-Teok yun, Associate Editor

*Keywords:*
Wetland
Oxbow hydrosystem
Surface/ground water interaction
Hydrochemistry
Stable isotopes

ABSTRACT

Wetlands as oxbows play a fundamental socio-economic and environmental role. They behave as efficient tools in regards to hydrological and ecological concerns: they contribute to control rivers discharge (flood prevention and contribution to drought flow) as well as to manage water quality (excess nutrients retention) and they constitute refuge habitats for flora and fauna. They may so become more and more determinant as nature-based solutions in a near future. However, the establishment of complete and reliable functioning models is complicated by the different connection degrees that can present these specific wetlands to the main stream and to the adjunct alluvial aquifer. Moreover, monodisciplinary approaches usually conducted can underestimate or even neglect sources of water supply. The present study offers a multidisciplinary approach coupling hydrodynamic (surface water/groundwater levels), geochemical (T, EC, pH, major ions) and isotopic ($\delta^2$H-$\delta^{18}$O) characterization in order to properly assess the dynamic of these specific hydrosystems and so be able to establish a complete and reliable hydrodynamic conceptual model. The coupling approach has been tested on the Auzon Oxbow, one of the fluvial annexes of the Allier River (Massif Central, France). The resulting conceptual model testifies for connection degree higher that expected between the oxbow and both the main stream and alluvial aquifer. Indeed, a non-negligible supply of the oxbow by the alluvial groundwater is observed, especially in its downstream part. As this part of the oxbow is the site of its confluence to the Allier River, groundwater supply could have been underestimated. The geochemical approach shows that Allier River also supply the oxbow through the upstream paleochannel, result of a channel migration 30 years ago. Hydrodynamic and isotopic approaches complete the understanding showing that the paleochannel pathway is only active during high flow periods (from November to June). Based on these results, the strategic utility of the proposed approach to study oxbow's hydrosystems has been proved.

## 1. Introduction

Wetlands were subject of various scientific considerations in recent decades and benefit from specific international convention especially as waterfowl habitat (Ramsar Convention, 1971). They are indeed particularly recognized to preserve the ecological function of hydrosystems (ecological niches, refuge areas…). However, during the last decades, the general intensification of pollution has led to the contamination of most of the water bodies with negative effects on aquatic ecosystems, human health, productive activities, water system reliability and operating costs for water use (Gleick, 1998; Bates et al., 2008; Hulton, 2012; Sutton et al., 2013; UNEP, 2016). In the meantime, a world loss of about 64–71% of natural wetlands is to deplore since 1900 because of human activities (Davidson, 2014). Locally, some sectors are especially affected with for instance percentage of wetlands lost reaching 91% for the California State between the 1780's and the 1980's (Dahl, 1990). Actions have been therefore implemented in order: 1) to preserve or restore wetlands, 2) to complete the knowledge on their functioning and 3) to communicate about the necessity of maintaining such environments. These are the objectives, for instance, of the 3rd

*Abbreviations:* GW, groundwater; RB, right bank; LB, left bank; T, water temperature

* Corresponding author at: GEOLAB UMR 6042 UBP & CNRS, 4 Rue Ledru, 63000 Clermont-Ferrand, France.
*E-mail address:* melanie.quenet@gmail.com (M. Quenet).

https://doi.org/10.1016/j.jhydrol.2019.123936
Received 20 February 2019; Received in revised form 3 July 2019; Accepted 8 July 2019
Available online 16 July 2019

National Action Plan for Wetlands in France (PNMH, 2014) and of the United States Geological Survey (Fretwell et al., 1996).

As a special feature of wetlands, oxbows are generated by spatial and temporal dynamics of rivers within their floodplains. That kind of perifluvial environments are of a major ecological importance for the habitat and diversity of fauna and vegetation. Oxbows indeed promote reproduction and provide refuge areas for biotic communities, especially fishes (Bornette et al., 1998; Ghosh and Biswas, 2017; Yang et al., 2018). However, since an oxbow is a floodplain annex, it can be supplied by local precipitation, main stream's water, alluvial groundwater from the bank between the river and the oxbow and from the bank delineating the alluvial plain (Rollet et al., 2005). Therefore, the whole ecosystem of oxbows depends largely on hydrodynamic conditions and more peculiarly on the mixing between water masses through hydrological connectivity to the main stream and/or the alluvial groundwater (Dahm et al., 1998; Amoros and Bornette, 2002). It is now widely recognized that maintaining oxbows in riparian areas contributes to control floods occurrence, to stabilize river base flows during dry periods, to enhance the water quality (by nutrient retention) and to preserve ecosystems (Winter et al., 1998; Alard et al., 2001; Bullock and Acreman, 2003; Larocque et al., 2016). However, obtain a complete hydrological knowledge about oxbows' dynamic remains challenging. Various monodisciplinary approaches implying mostly hydrodynamic but also hydrochemistry (Carrel and Juget, 1987; Bengen et al., 1992; Le Coz, 2003; Babka et al., 2011; Hudson et al., 2012) have been tested separately. However, such focused investigations can lead to neglect or underestimate contributions of connected water masses to the whole functioning of the oxbow which may produce unaccurate conceptual models to water managers. Multidisciplinary approach carried out on a representative and spatially distributed sampling network (boreholes and surface water points), covering both the selected wetland and the connected water masses of the whole hydrosystem, constitute an integrated solution to insure the most complete hydrological understanding of the system and therefore contribute effectively to wetlands and rivers preservation actions (restoration, rehabilitation, re-meandering…).

The present study is carried out on the Auzon Oxbow, one of the fluvial annexes of the Allier River (Massif Central, France, Fig. 1a), located in the upper Allier River basin. Ecological concerns surround that specific oxbow especially since it constitutes trout's reproduction and refuge areas. Consequently, local fishing associations carried out conservation operation as the dredging of alluvial plugs to maintain its connectivity to the main stream (Beauger et al., 2015). As an experimental site of the SOAHAL Observatory (Système d'Observation d'une Annexe Hydraulique de l'ALlier), a complete monitoring of the hydrosystem, including surface and groundwater with a dense spatial resolution (20 sampling sites for 0.4 $km^2$) has been organized from 2014. The objectives are to provide effective diagnostic tools to evaluate the connection degree of the Auzon Oxbow to the Allier River, the main stream, and to the adjunct alluvial aquifer and thus to establish a complete hydrodynamic description of the Auzon Oxbow hydrosystem. To achieve that goal, the strategy was to combine individual investigation approaches through a multidisciplinary analysis on both hydrodynamic and hydrochemistry.

## 2. Study area

### 2.1. General settings

The study was performed on the Auzon Oxbow (sexagesimal GPS standard longitude/latitude coordinates at the confluence: 03°21′41″E/45°22′05″N; elevation: 400 m), a fluvial annex of the Allier River, a gravel bed meandering stream located about 60 km southeast of Clermont-Ferrand, France. The Allier River originates at La Maure de Gardille (1423 m.a.s.l) and joins the Loire River at the Bec d'Allier near Nevers, after 410 km of course from South towards North within a 14,310 $km^2$ watershed (Fig. 1a). Allier River discharge at the station K2430810 of Agnat (Pont d'Auzon), located downstream of the study area at about 1500 m to the north (03°21′26″E/45°23′09″N; elevation: 360 m), ranges from 9.7 to 246.0 $m^3.s^{-1}$ with an annual average at 30.3 $m^3.s^{-1}$ (calculated over 26 years data; (Banque Hydro," n.d.)). The Auzon Oxbow is located in the first alluvial plain encountered downstream of the Allier Gorges. The study area presents a temperate continental climate with relatively hot summers (mean air temperatures up to 24 °C in July) and cold winters (mean temperatures around −3 °C in February; "Météo-France" n.d.). Annual precipitation is moderate within the Allier basin (692 mm on average), the valley being in a shelter position behind the western Massif Central where Atlantic humid air masses produce orographic rainfall; most of the events occur between May and October (423 mm in cumulative precipitation; "Météo-France" n.d.). Mountainous areas of the upper Allier catchment are more humid with a total precipitation around 2000 mm; minima are registered in the low Allier plain and account for around 570 mm/yr (Mohammed et al., 2014).

Geologically, the drainage basin of the Allier River is composed of 80% by crystalline formations (Hercynian crystalline bedrock and Cenozoic volcanic rocks), the remaining part of the watershed is made of calcareous Oligocene fluvio-lacustrine sediments (Korobova et al., 1997). The study area is located in the small subsidence basin of Brioude. That tectonic depression constitutes the western end of an E-W direction extension grabens network due to the tectonic phase in distention which took place in Western Europe during the Cenozoic period (Vanderhaeghe and Prognon, 2012). The Brioude basement is composed of Hercynian metamorphic and magmatic bedrock overlaid by the sedimentary formation of Limagne: during the Oligocene and Miocene periods, detrital sedimentation in continental environment (alternation of clays, sands and marls with some carbonates levels) filled the basin. Since Quaternary, the alluvial deposits of the Allier River are completing the sequence on the underlying Oligocene marls (Lasnier and Marchand, 1982; Korobova et al., 1997); they extend over a width of between 0.5 and 2 km and a thickness of about 10 m at the Auzon Oxbow site (alluvial plain of Fig. 1b). Due to their good hydrodynamic properties (Transmissivity = $10^{-3}$ à $10^{-4}$ $m^2$/s, Storage coefficient = 8–10%) and hydrochemical characteristics (moderate concentration, neutral pH and calcium-bicarbonate water-type) (Mohammed, 2014; Mohammed et al., 2014), the alluvial aquifer of the Allier River is one of the major water resources of the area. This aquifer is therefore intensively exploited for drinking water supply and agricultural purposes as it is the case on the study site.

Thanks to its geomorphology and location, Auzon Oxbow is considered as an active floodplain oxbow (Babka et al., 2011). It was formed by the migration of an old channel of the Allier River, which occurred during two flood events in 1988 and 1989. A former gravel pit located in the point bar has facilitated the cutoff process leading to the main channel abandon. Upper part of the channel was rapidly in-filled by sands and gravels; since then, only the downstream end remains connected to the main stream (Beauger, 2008) conferring to the Auzon Oxbow the first stage of development of oxbows (Gagliano and Howard, 1984; Wren et al., 2008; Hudson et al., 2012). As so, it can be supplied by water of four different origins: local precipitation, main stream's water through the confluence, groundwater inflowing from the bank between Allier River and the oxbow and finally, groundwater from the bank delineating the alluvial plain (Rollet et al., 2005). The 560 m length of the oxbow can be divided into three geomorphological parts (Fig. 1c):

- i) the upstream zone (UZ), which is disconnected from the main stream and is similar to a pond (197 m length, 13 m width and maximum depth of 1.8 m) ;
- ii) the intermediate zone (IZ), which is a former geomorphological riffle (176 m length, 0.3 to 8 m width and maximum depth of 0.4 m) ;

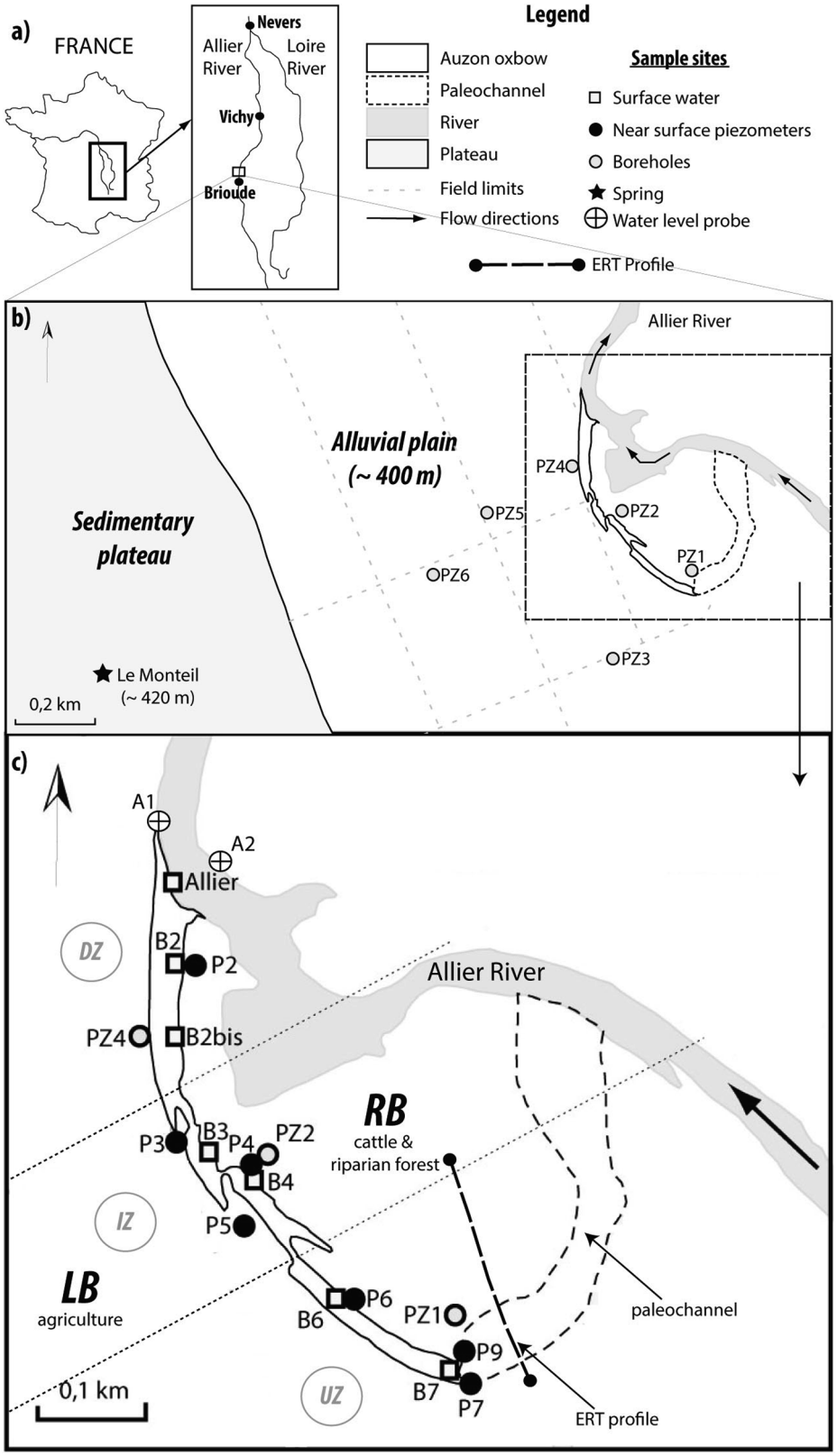


**Fig. 1.** a) Location of the Auzon Oxbow; b) Location of the SOAHAL Observatory with c) a zoom on the Auzon Oxbow (the two small dashed lines delineate the three distinct sections of the oxbow: UZ (upstream zone), IZ (intermediate zone) and DZ (downstream zone)).

- iii) and the downstream zone (DZ), which is connected to the Allier River by its downstream extremity (Beauger et al., 2015) (188 m length, 17 m width and maximum depth of 1.6 m).

Highly subject to flooding, the right bank (RB) is used for punctual grazing while the left bank (LB) is a low terrace dedicated to cereals production. However, close to the Auzon Oxbow, crops are smaller and agricultural practices relatively soft compared to the western plateau

where they are much more intensive (Fig. 1b). That neighboring plateau presents an aquifer that is assumed to partly feed the LB alluvial groundwater. Auzon Oxbow has been monitored since 2007 (Beauger, 2008) in terms of geomorphology, sedimentation and ecology (study of diatom, macrophyte and benthic macroinvertebrate communities). To complete ecological investigations, the monitoring has been extended to surface and groundwater hydrodynamic and hydrochemistry. In this purpose, near-surface piezometers (from 0.92 to 1.85 m deep) were built on the oxbow's shore of both banks (Fig. 1c) in 2012 (Beauger et al., 2015) as well as deep observation boreholes catching the whole aquifer thickness in 2014.

### 2.2. Sampling sites

Precipitation height have been collected from Météo-France database at Sainte-Florine, the closest weather station, located 4 km northwest (03°19′00'E/45°24′00″N; elevation: 450 m; station 43185001) and at Naussac (03°49′42″E/44°44′54″N; elevation: 967 m; station 48105001), weather station characterizing the upper part of the Allier watershed. Allier River daily discharge is taken from the Agnat-Pont d'Auzon station (Banque Hydro," n.d.).

In addition, monthly monitoring is performed at the following sites in the area (Fig. 1): i) 6 surface water observation points distributed along the entire Auzon Oxbow from its upstream to its downstream ends (B2 to B7); ii) 1 surface water observation point in the Allier River (Allier); iii) 6 observation boreholes (10 m deep covering the entire alluvial aquifer thickness), 2 drilled in the Right Bank (RB: PZ1 and PZ2) and 4 in the Left Bank (LB: PZ3 to PZ6); iv) 7 near-surface piezometers (0.85 to 1.92 m deep), located next to the oxbow on both RB and LB (P2 to P9); v) Le Monteil spring (Fig. 1b) draining the neighboring plateau aquifer, which is assumed to partly feed the alluvial groundwater.

## 3. Sampling and analytical methods

### 3.1. Hydrodynamic monitoring [07/22/2014 – 11/24/2017]

In order to assess the hydrodynamic behavior of the oxbow, the potential water sources entering the system have been investigated in terms of hydrodynamic and hydrochemistry. Surface water level of the Allier River at the confluence with the Auzon Oxbow and water table in the 6 observation boreholes have been recorded on an hourly basis with an *in situ* Level Troll 500 probe. All water level data have been corrected from the barometric pressure variations. The hydrological station was located on LB prior to the 11/05/2015 (A1, Fig. 1c) and then moved to RB (A2, Fig. 1c) because of a too important erosion of the left bank during previous floods. Geographical coordinates and elevation of each pressure sensor were measured using the centimetric Trimble R10 DGPS whose data was post-processed with Trimble Business Center software (version 3.8.) and adjusted according to the dimensions of the boreholes in order to calculate level variations through time in the same reference of altitude (Cunningham and Schalk, 2011). The reliability of the continuous piezometric levels monitoring was checked and validated through manual measurements carried out during the 40 sampling campaigns: correlation coefficients between data recorded and manually measured ($r^2$ from 0.92 to 0.99) testify for a good representativeness of the piezometric level time-series.

### 3.2. Water chemistry monitoring

Forty sampling campaigns have been performed on the 21 sampling sites on a monthly basis from July 2014 to November 2017, except in February 2017 when the alluvial plain was flooded. A few data are also missing for P7, because of small floods or vandalism. Prior to sampling, bottles have been rinsed two times by using the water to be sampled. Surface waters and Le Monteil spring were directly sampled using sampling vials. Groundwater was sampled using a Cole Parmer Masterflex I/S pump for near-surface piezometers, while it was a 12 V standard PVC narrow diameter submersible pump for the observation boreholes. For each groundwater sampling, stagnating water present into the borehole was renewed before sampling and measuring. An intensive campaign was performed on the 23rd of November 2017 in the Auzon Oxbow in order to assess spatial distribution of electrical conductivity (EC): 124 measures have been performed in the near surface of the oxbow (0.2 m depth) along the UZ, the IZ and on the upper part of the DZ, using a WTW multi 340i and a DGPS Trimble Geo7x whose data were post-processed with Pathfinder software. Two sites of the EC campaign (Points 3 and 103) were also sampled for major ions analyses. EC, pH and water temperature have been measured *in situ* using a WTW multi 340i. $HCO_3^-$ concentrations have been determined directly in the field by using HACH Digital Titrator, sulfuric acid (0.1600 N and 1.600 N) and Bromocresol Green-Methyl Red Indicator (Hach method 8203).

A total of 837 water samples have thus been taken in clean sterile polypropylene straight containers with polyethylene caps of 180 mL, transported in cooler to GEOLAB laboratory in Clermont-Ferrand (CNRS UMR 6042, University Clermont-Auvergne) and then stored at 4 °C. Anions and cations were analyzed within 3 days in GEOLAB Laboratory: anions ($F^-$, $Cl^-$ $NO_2^-$, $NO_3^-$, $PO_4^{3-}$, $SO_4^{2-}$) using the Thermo Fisher Scientific Dionex DX120 ionic chromatography with a Ionpac AS23 4*250 mm column and the Dionex 7 anions standard solution; cations ($Li^+$, $Na^+$, $NH_4^+$, $K^+$, $Mg^{2+}$, $Ca^{2+}$) using the Thermo Fisher Scientific Dionex ICS1100 ionic chromatography with a Ionpac CS12A 4*250 mm column and the Dionex 6 cations standard solution. The error margins were of ± 4–6% and ± 2–4% respectively for anions and cations. These analyses are reliable since all the 839 ionic balances (837 monthly + punctual samples 3 and 103) are under 10% with even 95.1% under 5%.

From July 2014 to March 2017, only groundwater from the six observation boreholes has been analyzed for stable isotopes. Since April 2017, all sites have been sampled for $\delta^2H$ and $\delta^{18}O$ analyses, so the database accounts for 360 isotopic analyses. Waters have been collected with no air bubbles, in 20 mL borosilicate glass vials closed by polypropylene caps. Isotopic analysis were performed at the University of Corsica, France (CNRS UMR 6134 SPE): both $^2H$ and $^{18}O$ of the water molecule were characterized using a liquid-water stable isotope analyzer DLT-100 (Los Gatos Research) according to the analytical scheme recommended by the IAEA (IAEA, 2009; Penna et al., 2010). Isotopic data were reported in the standard delta notation in part per thousand relative to Vienna Standard Mean Ocean Water (VSMOW; (Clark and Fritz, 1997)). The accuracy is 1‰ for $\delta^2H$ and 0.1‰ for $\delta^{18}O$.

### 3.3. Geophysical investigations

Electrical Resistivity Tomography (ERT) is a geophysical method providing images of electrical resistivity ρ (inverse of conductivity) of the subsurface. ERT is generally used to characterize the lithology and the geometry of the ground, to assess its saturation, or even to monitor soil pollution (Loke, 2011). The technique consists of injecting current in a pair of electrodes set into the ground and measuring the resulting potential difference between another dipole of electrodes which yields information about ρ.

A 2D ERT survey was carried out on the SOAHAL Observatory on the 02/21/2018 in order to investigate potential underground connections between Auzon Oxbow and Allier River. The data collection was done by using a SYSCAL R1 + (Iris instruments), with a Wenner-Schlumberger electrode configuration (Loke and Barker, 1996). An array of 72 electrodes was installed, distributed every 3 m, along a NNW-SSE line (Fig. 1c). The apparent resistivity data were inverted with RES2DINV software (Loke, 2016) using least-squares inversion optimization. Inversion converged to RMS error of 3% after 5 iterations.

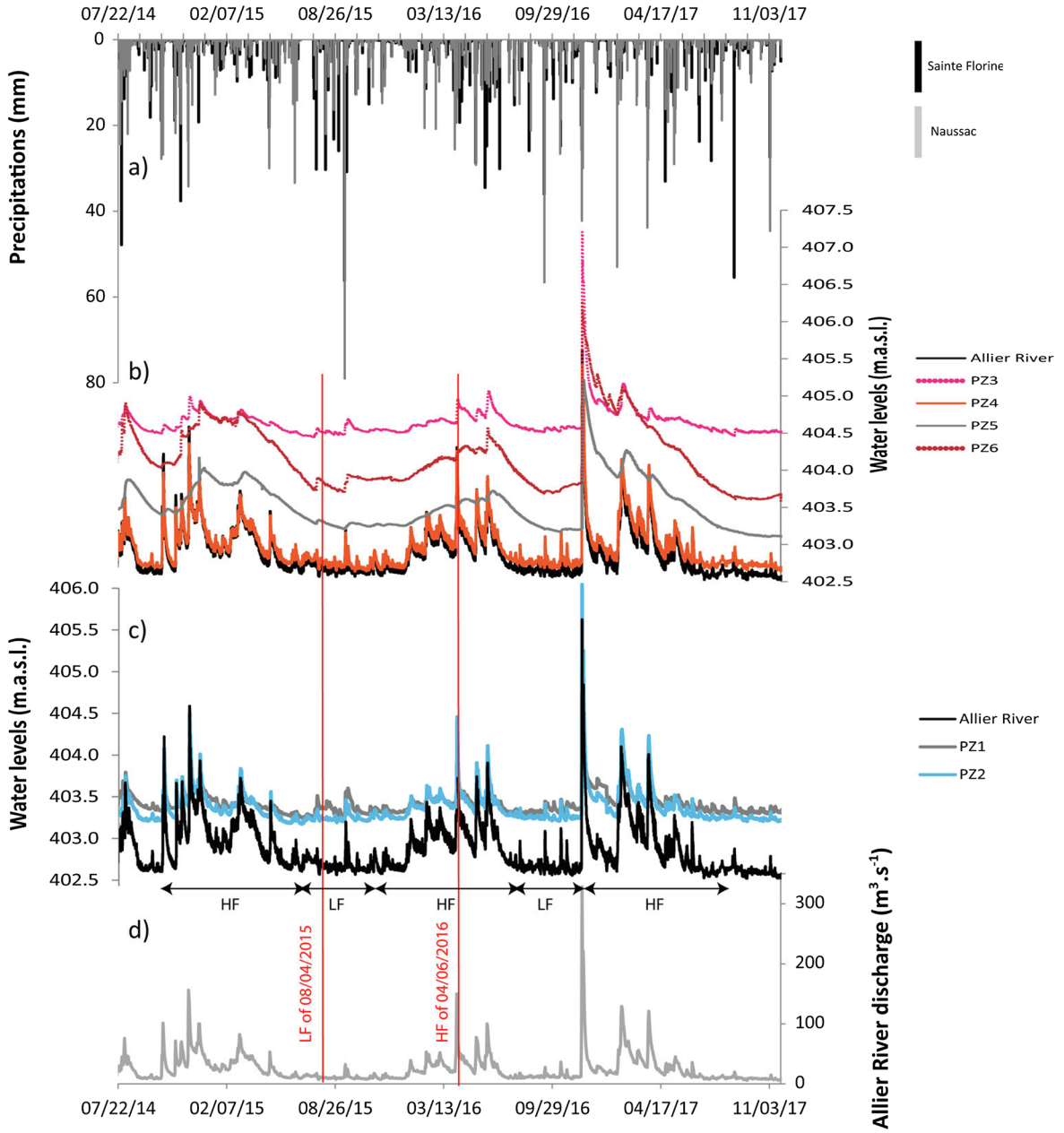


**Fig. 2.** Time-series of a) Daily precipitation at Sainte Florine (Météo-France station 43185001, altitude 450 m) and Naussac (Météo-France station 48105001, altitude 967 m); b) and c) surface water level at the confluence between Auzon Oxbow and Allier River; groundwater levels at boreholes b) PZ3 to PZ6 (LB) and c) PZ1 and PZ2 (RB); d) Allier River discharge at Agnat-Pont d'Auzon station (from Banque Hydro). Low-flow (LF) and high-flow (HF) are identified with black double arrows while 08/04/2015 and 04/06/2016 events are identified with red lines. (For interpretation of the references to colour in this figure legend, the reader is referred to the web version of this article.)

## 4. Results and discussion

### 4.1. End-members characterization and interactions

#### 4.1.1. Hydrodynamical data

Allier River discharge presents an average value of 25 $m^3.s^{-1}$ for the studied period (07/22/2014 – 11/24/2017). The most important flood impulse reached 328 $m^3.s^{-1}$ (11/23/2016) while two other flood peaks have been registered equal or superior to 150 $m^3.s^{-1}$ (156 $m^3.s^{-1}$ on the 11/29/2014 and 150 $m^3.s^{-1}$ on the 04/06/16; Fig. 2d). These events are quite moderate compared to the large floods that Allier River can historically experience (10Y-flood and 50Y-flood: 590 and 840 $m^3.s^{-1}$ respectively; Banque Hydro," n.d.). Annual discharge variations are observed with globally low flow (LF) periods during the warmest months (from July to October) with an average flow rate around 14 $m^3.s^{-1}$ while high flow (HF) periods including important flood events occur along the rest of the year with an average flow rate around 32 $m^3.s^{-1}$. This LF-HF distribution over time is more consistent with variations of precipitation recorded in the upstream mountainous area (Mohammed et al., 2014), whose Naussac weather station is the witness (Fig. 2a), than the local ones (represented by Sainte-Florine weather station on Fig. 2a). However, the maximum flood peak of 328 $m^3.s^{-1}$ is actually related to high precipitation recorded at both stations, suggesting a generalized rainfall event linked to a Cevénol episode (a climatic phenomenon more and more frequent these last few years with rainy events that mainly affects the Cevennes' mountain range and piedmont which often cause severe floods in the Massif Central Region) (Jubertie, 2006; Gay, 2015). On the contrary, flood

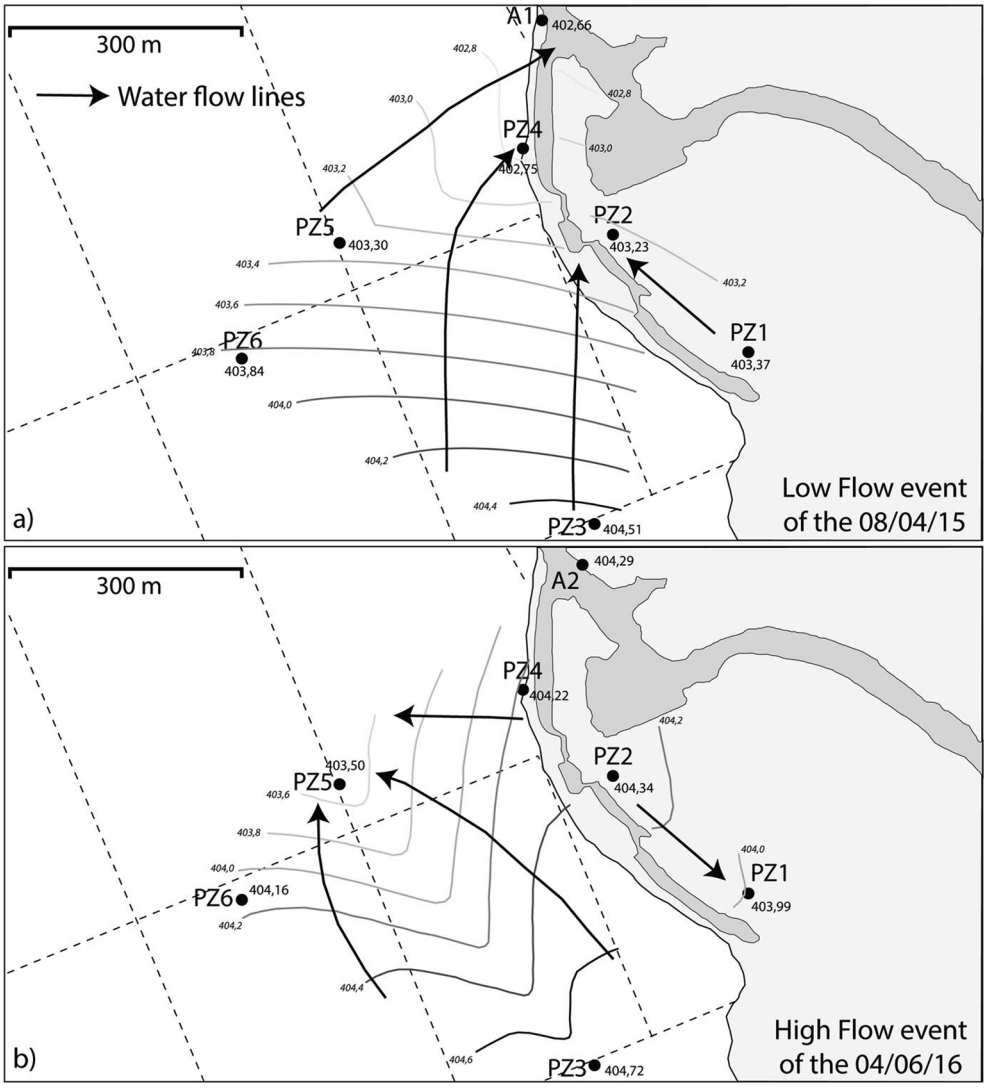


**Fig. 3.** Piezometric maps a) of the Low Flow (LF) event of the 08/04/2015 and; b) of the High Flow (HF) event of the 04/06/2016.

peak occurring the 01/26/2017 seems to be only due to high altitude precipitation: rainfall event is actually only recorded at Naussac weather station. Finally, flood peak recorded the 08/30/2017 is caused by a stormy event affecting Saint-Florine weather station only. These examples emphasize that discharge variations recorded for Allier River are related to a large set of meteorological conditions affecting the entire Allier basin, including rapid winter temperature elevation with or without rainfall causing snow melting (Jubertie, 2006).

Water level variations at the Auzon Oxbow/Allier River confluence (solid black lines in Fig. 2b and c) are consistent with discharge variations of the Allier River recorded at Agnat-Pont d'Auzon station (Fig. 2d). It shows the accuracy of the *in situ* surface water level monitoring which was therefore crossed with water table monitoring for piezometric mapping (triangular interpolation). Fig. 3a and b present LF (08/04/2015) and HF (04/06/2016) piezometric maps, respectively. These two dates are identified on Fig. 2d. The LF piezometric map indicates a global northward circulation of groundwater (GW) and identified GW as a potential end-member supplying Auzon Oxbow. Water level time-series observation (Fig. 2b and c) shows that PZ1 and PZ2 (RB) as well as PZ4 (LB) present very impulsive variations. They were pretty close to the water level variations at the confluence Auzon Oxbow/Allier River. Moreover, in HF, piezometric levels were lower than surface water levels with 0.7% of the records at PZ1, 0.3% at PZ2 and 4% at PZ4. This observation suggests that GW are supplied by surface water, whatever bank considered, during HF. PZ3, PZ5 and PZ6 (LB) show smoother signals (Fig. 2b); most of the LB piezometric level variations remained consistent with the surface water level variations.

The HF piezometric map illustrates the hydrodynamic situation during the third most important flood event of the studied period. This flood was linked to a large rainfall event which affected the whole Allier River catchment (Fig. 2a). The map can be used to identify potential hydrodynamic changes compared to LF situation. Then an inversion of the hydraulic gradient is induced by high surface water level recorded at the Auzon Oxbow/Allier River confluence; it affects GW on both Auzon Oxbow banks. However, in the RB, inversion is reduced to a GW flow inversion (from PZ2 to PZ1) since the Allier River discharge just began to decline while the RB is still in charge. On the LB, inversion seemed to extend from surface water to PZ5 passing through PZ4. Actually, during that HF event as generally for all HF recordings, PZ4 levels varied synchronously with the surface water level up to inversion of hydraulic gradient while the other LB boreholes remained stable, PZ5 included. PZ3 piezometric level starts to increase only 24 h after the rise of surface water level, the response delay of PZ5 and PZ6 is about 26 h. Besides, PZ5 piezometric level stays lower than the one of PZ6, inducing a piezometric depression. The delay between the increase in surface water level and that of the more inland LB boreholes suggests that the hydraulic gradient inversion is limited to PZ4. This hydrodynamic feature can be explained by high disparities existing within the alluvial

**Table 1**
Average, minimum, maximum and standard deviation (SD) values of physico-chemical parameters, ions concentrations and $\delta^{18}O$-$\delta^{2}H$ data for the 40 campaigns carried out at the 21 samples sites of the study zone.

| Sample ID | | T | pH | EC | $HCO_3^-$ | $Cl^-$ | $SO_4^{2-}$ | $NO_3^-$ | $NO_2^-$ | $PO_4^{3-}$ | $F^-$ | $Na^+$ | $Ca^{2+}$ | $Mg^{2+}$ | $K^+$ | $NH_4^+$ | $Li^+$ | $\delta^2H$ | $\delta^{18}O$ |
|---|---|---|---|---|---|---|---|---|---|---|---|---|---|---|---|---|---|---|---|
| | | (°C) | | ($\mu S.cm^{-1}$) | ($mg.l^{-1}$) | | | | | | | | | | | | | (‰ VSMOW) | |
| Allier | Av. | 12.3 | 7.6 | 110 | 30.2 | 9.9 | 6.1 | 3.2 | 0.0 | 0.1 | 0.1 | 7.1 | 7.7 | 3.2 | 1.6 | 0.1 | 0.0 | −52.0 | −8.0 |
| | Min. | 0.9 | 7.0 | 62 | 12.5 | 5.4 | 3.8 | 1.2 | 0.0 | 0.0 | 0.0 | 3.9 | 4.4 | 1.7 | 1.0 | 0.0 | 0.0 | −56.7 | −8.8 |
| | Max. | 21.8 | 8.8 | 152 | 49.0 | 14.7 | 10.3 | 6.7 | 0.0 | 0.1 | 0.3 | 9.6 | 11.8 | 4.9 | 2.6 | 0.2 | 0.0 | −47.5 | −7.1 |
| | SD | 6.0 | 0.4 | 17 | 7.8 | 2.0 | 1.3 | 1.4 | 0.0 | 0.0 | 0.0 | 1.2 | 1.5 | 0.7 | 0.3 | 0.0 | 0.0 | 3.4 | 0.6 |
| B2 | Av. | 12.6 | 7.4 | 242 | 77.2 | 19.8 | 12.1 | 2.1 | 0.0 | 0.1 | 0.1 | 11.1 | 21.1 | 7.4 | 2.6 | 0.1 | 0.0 | −51.4 | −7.8 |
| | Min. | 1.1 | 6.9 | 76 | 16.7 | 6.6 | 5.0 | 0.2 | 0.0 | 0.0 | 0.1 | 4.7 | 5.1 | 2.0 | 1.5 | 0.0 | 0.0 | −55.7 | −8.6 |
| | Max. | 22.8 | 8.0 | 483 | 180.0 | 38.0 | 25.6 | 6.7 | 0.1 | 0.1 | 0.2 | 17.9 | 47.3 | 19.3 | 4.5 | 0.4 | 0.0 | −47.4 | −7.2 |
| | SD | 5.7 | 0.2 | 123 | 46.9 | 8.5 | 5.9 | 1.5 | 0.0 | 0.0 | 0.0 | 3.9 | 12.4 | 4.5 | 0.8 | 0.1 | 0.0 | 3.0 | 0.5 |
| B2bis | Av. | 12.3 | 7.2 | 362 | 116.1 | 31.6 | 17.2 | 1.9 | 0.0 | 0.1 | 0.2 | 16.0 | 34.0 | 10.2 | 4.0 | 0.1 | 0.0 | −51.9 | −7.9 |
| | Min. | 4.7 | 6.7 | 116 | 29.3 | 9.7 | 6.5 | 0.2 | 0.0 | 0.0 | 0.1 | 6.3 | 8.8 | 3.0 | 2.1 | 0.0 | 0.0 | −52.9 | −8.0 |
| | Max. | 18.4 | 7.9 | 452 | 151.0 | 48.7 | 31.4 | 8.0 | 0.1 | 0.1 | 0.3 | 20.5 | 48.3 | 15.9 | 20.7 | 0.2 | 0.0 | −48.0 | −7.5 |
| | SD | 3.9 | 0.2 | 63 | 24.1 | 8.2 | 5.1 | 1.8 | 0.0 | 0.0 | 0.0 | 2.9 | 7.8 | 2.3 | 2.9 | 0.1 | 0.0 | 1.6 | 0.2 |
| B3 | Av. | 12.3 | 7.2 | 337 | 111.9 | 31.2 | 15.4 | 1.7 | 0.0 | 0.1 | 0.2 | 16.5 | 32.0 | 9.3 | 4.0 | 0.1 | 0.0 | −52.6 | −8.0 |
| | Min. | 5.5 | 6.8 | 140 | 42.0 | 12.6 | 7.4 | 0.2 | 0.0 | 0.0 | 0.1 | 7.8 | 11.1 | 3.5 | 2.7 | 0.0 | 0.0 | −53.4 | −8.1 |
| | Max. | 21.3 | 7.7 | 462 | 155.0 | 51.6 | 30.9 | 7.6 | 0.2 | 0.1 | 0.3 | 20.6 | 50.1 | 14.8 | 24.0 | 0.3 | 0.0 | −52.0 | −7.9 |
| | SD | 3.9 | 0.2 | 65 | 19.7 | 8.4 | 5.4 | 1.9 | 0.0 | 0.0 | 0.0 | 2.6 | 6.7 | 2.0 | 3.3 | 0.1 | 0.0 | 0.5 | 0.1 |
| B4 | Av. | 12.3 | 7.1 | 337 | 111.1 | 30.4 | 14.9 | 1.9 | 0.0 | 0.1 | 0.2 | 16.5 | 31.8 | 9.1 | 3.5 | 0.1 | 0.0 | −52.4 | −7.9 |
| | Min. | 6.0 | 6.8 | 155 | 43.0 | 13.7 | 8.2 | 0.3 | 0.0 | 0.0 | 0.1 | 8.4 | 12.4 | 3.9 | 2.6 | 0.0 | 0.0 | −53.2 | −8.1 |
| | Max. | 20.9 | 7.9 | 425 | 133.0 | 44.6 | 25.9 | 7.6 | 0.1 | 0.2 | 0.3 | 20.8 | 40.5 | 11.7 | 4.1 | 0.3 | 0.0 | −51.0 | −7.7 |
| | SD | 3.3 | 0.2 | 57 | 17.1 | 7.4 | 4.3 | 1.8 | 0.0 | 0.0 | 0.0 | 2.6 | 6.0 | 1.6 | 0.3 | 0.1 | 0.0 | 0.8 | 0.2 |
| B6 | Av. | 13.3 | 7.1 | 302 | 98.3 | 27.0 | 12.2 | 1.5 | 0.0 | 0.1 | 0.2 | 15.5 | 27.1 | 7.6 | 3.4 | 0.1 | 0.0 | −52.5 | −7.9 |
| | Min. | 6.6 | 6.7 | 210 | 53.0 | 17.0 | 7.3 | 0.1 | 0.0 | 0.0 | 0.1 | 11.4 | 16.4 | 5.3 | 2.7 | 0.0 | 0.0 | −53.7 | −8.2 |
| | Max. | 21.0 | 8.3 | 431 | 135.0 | 51.2 | 22.0 | 6.7 | 0.0 | 0.2 | 0.2 | 22.0 | 40.1 | 13.3 | 4.6 | 0.2 | 0.0 | −50.8 | −7.4 |
| | SD | 3.3 | 0.3 | 49 | 16.0 | 7.3 | 3.9 | 1.5 | 0.0 | 0.0 | 0.0 | 2.6 | 5.3 | 1.6 | 0.4 | 0.1 | 0.0 | 0.9 | 0.2 |
| B7 | Av. | 12.8 | 7.0 | 215 | 69.7 | 19.3 | 8.4 | 2.3 | 0.0 | 0.1 | 0.1 | 12.2 | 18.7 | 5.1 | 2.7 | 0.1 | 0.0 | −53.1 | −8.1 |
| | Min. | 8.6 | 6.6 | 157 | 50.0 | 10.2 | 5.7 | 0.8 | 0.0 | 0.0 | 0.1 | 9.3 | 13.8 | 3.8 | 2.1 | 0.0 | 0.0 | −54.8 | −8.2 |
| | Max. | 18.3 | 7.6 | 373 | 95.0 | 28.8 | 13.5 | 9.0 | 0.0 | 0.5 | 0.2 | 16.5 | 25.8 | 6.8 | 5.0 | 0.2 | 0.0 | −50.4 | −7.7 |
| | SD | 2.0 | 0.2 | 37 | 10.0 | 5.1 | 2.0 | 1.5 | 0.0 | 0.1 | 0.0 | 1.9 | 2.6 | 0.7 | 0.5 | 0.1 | 0.0 | 1.3 | 0.2 |
| Monteil | Av. | 13.1 | 7.2 | 925 | 235.5 | 66.1 | 69.8 | 97.9 | 0.0 | 0.5 | 0.4 | 14.0 | 125.3 | 18.4 | 15.6 | 0.1 | 0.0 | −50.0 | −7.3 |
| | Min. | 9.5 | 7.0 | 871 | 134.0 | 55.1 | 60.8 | 87.0 | 0.0 | 0.0 | 0.3 | 12.3 | 74.1 | 16.8 | 10.6 | 0.0 | 0.0 | −50.6 | −7.5 |
| | Max. | 16.2 | 7.5 | 1031 | 273.0 | 97.3 | 87.3 | 120.6 | 0.1 | 4.1 | 0.6 | 18.4 | 145.6 | 25.1 | 47.0 | 0.3 | 0.0 | −49.4 | −7.2 |
| | SD | 1.7 | 0.1 | 39 | 26.9 | 9.3 | 4.7 | 7.5 | 0.0 | 0.6 | 0.1 | 1.2 | 13.5 | 1.5 | 7.7 | 0.1 | 0.0 | 0.4 | 0.1 |
| P2 | Av. | 12.8 | 6.9 | 230 | 77.6 | 15.2 | 12.0 | 3.2 | 0.0 | 0.0 | 0.2 | 13.3 | 13.8 | 9.3 | 3.0 | 0.0 | 0.0 | −54.8 | −8.4 |
| | Min. | 4.9 | 6.5 | 147 | 34.0 | 8.5 | 3.1 | 0.0 | 0.0 | 0.0 | 0.1 | 7.7 | 7.5 | 5.4 | 1.4 | 0.0 | 0.0 | −55.9 | −8.6 |
| | Max. | 20.1 | 7.9 | 357 | 131.0 | 38.7 | 28.3 | 10.5 | 0.0 | 0.1 | 0.3 | 19.0 | 25.3 | 17.9 | 14.6 | 0.2 | 0.0 | −54.0 | −8.2 |
| | SD | 3.7 | 0.3 | 59 | 24.1 | 7.2 | 6.2 | 3.0 | 0.0 | 0.0 | 0.0 | 3.0 | 4.7 | 2.9 | 3.2 | 0.0 | 0.0 | 0.6 | 0.2 |
| P3 | Av. | 12.5 | 7.1 | 744 | 238.5 | 53.1 | 61.0 | 26.0 | 0.0 | 0.1 | 0.3 | 17.3 | 80.8 | 28.2 | 4.2 | 0.0 | 0.0 | −50.6 | −7.6 |
| | Min. | 7.6 | 6.9 | 215 | 66.0 | 13.8 | 13.7 | 11.1 | 0.0 | 0.1 | 0.1 | 8.7 | 19.9 | 6.8 | 1.8 | 0.0 | 0.0 | −51.2 | −7.7 |
| | Max. | 17.3 | 7.4 | 950 | 293.0 | 101.0 | 105.0 | 46.1 | 0.1 | 0.7 | 0.4 | 23.5 | 102.1 | 39.8 | 7.0 | 0.2 | 0.0 | −49.9 | −7.5 |
| | SD | 2.5 | 0.2 | 101 | 34.1 | 12.9 | 12.1 | 6.8 | 0.0 | 0.1 | 0.1 | 2.1 | 13.9 | 4.4 | 0.7 | 0.0 | 0.0 | 0.4 | 0.1 |
| P4 | Av. | 12.8 | 7.0 | 381 | 139.4 | 32.7 | 7.3 | 0.2 | 0.0 | 0.0 | 0.2 | 17.0 | 34.9 | 10.6 | 3.5 | 0.9 | 0.0 | −52.1 | −7.9 |
| | Min. | 5.1 | 6.7 | 287 | 101.0 | 21.7 | 0.1 | 0.0 | 0.0 | 0.0 | 0.1 | 13.0 | 26.1 | 7.5 | 2.5 | 0.1 | 0.0 | −52.5 | −8.0 |
| | Max. | 19.2 | 7.7 | 587 | 203.0 | 45.5 | 42.2 | 0.9 | 0.0 | 0.1 | 0.3 | 22.8 | 62.0 | 18.9 | 4.7 | 1.9 | 0.0 | −51.4 | −7.8 |
| | SD | 3.7 | 0.2 | 71 | 22.6 | 7.7 | 10.5 | 0.2 | 0.0 | 0.0 | 0.0 | 2.5 | 7.9 | 2.7 | 0.5 | 0.4 | 0.0 | 0.4 | 0.1 |
| P5 | Av. | 12.6 | 7.1 | 795 | 255.4 | 59.8 | 65.3 | 20.4 | 0.0 | 0.2 | 0.2 | 20.0 | 87.9 | 29.1 | 3.1 | 0.0 | 0.0 | −50.8 | −7.6 |
| | Min. | 9.2 | 7.0 | 575 | 166.0 | 46.1 | 41.4 | 13.3 | 0.0 | 0.0 | 0.1 | 17.1 | 52.4 | 18.6 | 2.1 | 0.0 | 0.0 | −51.6 | −7.9 |
| | Max. | 15.5 | 7.7 | 859 | 295.0 | 70.0 | 73.8 | 34.4 | 0.1 | 0.8 | 0.3 | 23.1 | 104.0 | 39.0 | 4.8 | 0.1 | 0.0 | −50.4 | −7.5 |
| | SD | 1.8 | 0.1 | 48 | 26.0 | 5.8 | 5.2 | 5.2 | 0.0 | 0.2 | 0.0 | 1.3 | 12.9 | 2.7 | 0.4 | 0.0 | 0.0 | 0.4 | 0.1 |
| P6 | Av. | 13.2 | 7.1 | 396 | 126.7 | 37.9 | 17.0 | 1.7 | 0.0 | 0.1 | 0.2 | 21.1 | 37.1 | 9.3 | 4.6 | 0.0 | 0.0 | −53.1 | −8.0 |
| | Min. | 5.7 | 6.7 | 253 | 74.0 | 21.0 | 9.3 | 0.0 | 0.0 | 0.0 | 0.1 | 14.6 | 24.0 | 6.0 | 2.5 | 0.0 | 0.0 | −54.4 | −8.3 |
| | Max. | 19.4 | 7.8 | 495 | 163.0 | 58.7 | 33.6 | 6.5 | 0.1 | 0.4 | 0.3 | 29.6 | 47.7 | 15.4 | 14.3 | 0.2 | 0.0 | −52.0 | −7.8 |
| | SD | 3.2 | 0.2 | 54 | 17.0 | 9.4 | 5.0 | 1.5 | 0.0 | 0.1 | 0.0 | 3.5 | 5.5 | 1.8 | 1.9 | 0.0 | 0.0 | 0.8 | 0.1 |
| P7 | Av. | 13.3 | 6.9 | 219 | 69.5 | 20.6 | 8.2 | 2.4 | 0.0 | 0.3 | 0.2 | 12.9 | 19.1 | 5.2 | 3.2 | 0.0 | 0.0 | −53.4 | −8.2 |
| | Min. | 8.0 | 6.6 | 163 | 52.0 | 10.5 | 5.6 | 0.2 | 0.0 | 0.0 | 0.1 | 9.1 | 14.1 | 3.4 | 2.1 | 0.0 | 0.0 | −54.7 | −8.4 |
| | Max. | 20.5 | 7.7 | 316 | 91.0 | 48.5 | 12.9 | 7.5 | 0.1 | 0.8 | 0.2 | 18.9 | 24.2 | 9.5 | 23.5 | 0.1 | 0.0 | −51.2 | −7.8 |
| | SD | 2.5 | 0.3 | 34 | 9.1 | 8.0 | 1.9 | 1.4 | 0.0 | 0.2 | 0.0 | 2.5 | 2.5 | 1.1 | 3.4 | 0.0 | 0.0 | 1.1 | 0.2 |
| P9 | Av. | 12.9 | 6.9 | 335 | 113.6 | 33.7 | 9.7 | 0.4 | 0.0 | 0.1 | 0.2 | 19.2 | 31.7 | 6.5 | 5.3 | 0.1 | 0.0 | −53.3 | −8.1 |
| | Min. | 6.6 | 6.6 | 203 | 70.0 | 15.9 | 3.9 | 0.0 | 0.0 | 0.0 | 0.2 | 11.1 | 19.7 | 4.2 | 2.6 | 0.0 | 0.0 | −54.6 | −8.5 |
| | Max. | 18.8 | 7.3 | 498 | 167.0 | 98.8 | 23.8 | 4.3 | 0.0 | 0.2 | 0.3 | 31.3 | 48.9 | 9.3 | 63.1 | 0.3 | 0.0 | −51.3 | −7.7 |
| | SD | 2.9 | 0.2 | 83 | 28.3 | 16.7 | 4.2 | 0.8 | 0.0 | 0.0 | 0.0 | 5.6 | 8.3 | 1.7 | 9.4 | 0.1 | 0.0 | 1.2 | 0.3 |
| PZ1 | Av. | 13.1 | 7.1 | 290 | 95.8 | 28.3 | 11.3 | 0.8 | 0.0 | 0.1 | 0.2 | 16.3 | 27.3 | 6.4 | 4.0 | 0.1 | 0.0 | −53.7 | −8.1 |
| | Min. | 7.1 | 6.7 | 193 | 64.0 | 11.1 | 5.5 | 0.1 | 0.0 | 0.0 | 0.1 | 10.7 | 16.6 | 4.1 | 2.5 | 0.0 | 0.0 | −57.7 | −8.5 |
| | Max. | 19.1 | 7.6 | 413 | 131.0 | 82.0 | 35.1 | 4.0 | 0.0 | 0.2 | 0.3 | 25.5 | 43.9 | 10.4 | 25.1 | 0.2 | 0.0 | −49.8 | −7.5 |
| | SD | 2.8 | 0.2 | 73 | 18.4 | 15.4 | 6.8 | 1.0 | 0.0 | 0.0 | 0.0 | 3.9 | 7.7 | 1.9 | 3.5 | 0.1 | 0.0 | 1.7 | 0.3 |

(*continued on next page*)

**Table 1** (*continued*)

| Sample ID | | T | pH | EC | $HCO_3^-$ | $Cl^-$ | $SO_4^{2-}$ | $NO_3^-$ | $NO_2^-$ | $PO_4^{3-}$ | $F^-$ | $Na^+$ | $Ca^{2+}$ | $Mg^{2+}$ | $K^+$ | $NH_4^+$ | $Li^+$ | $\delta^2H$ | $\delta^{18}O$ |
|---|---|---|---|---|---|---|---|---|---|---|---|---|---|---|---|---|---|---|---|
| | | (°C) | | ($\mu S.cm^{-1}$) | ($mg.l^{-1}$) | | | | | | | | | | | | | (‰ VSMOW) | |
| PZ2 | Av. | 12.9 | 7.1 | 491 | 167.4 | 40.0 | 23.4 | 1.3 | 0.0 | 0.1 | 0.2 | 17.7 | 48.6 | 14.9 | 4.0 | 0.3 | 0.0 | −52.0 | −7.8 |
| | Min. | 7.2 | 6.8 | 325 | 114.0 | 24.2 | 4.8 | 0.1 | 0.0 | 0.0 | 0.1 | 13.0 | 30.6 | 8.9 | 2.8 | 0.0 | 0.0 | −53.2 | −8.1 |
| | Max. | 21.3 | 7.4 | 708 | 233.0 | 64.6 | 52.3 | 4.8 | 0.1 | 0.1 | 0.3 | 23.3 | 75.0 | 22.9 | 16.3 | 1.0 | 0.0 | −50.8 | −7.4 |
| | SD | 3.3 | 0.1 | 99 | 28.5 | 10.4 | 12.0 | 1.4 | 0.0 | 0.0 | 0.0 | 2.5 | 11.8 | 3.7 | 2.1 | 0.2 | 0.0 | 0.6 | 0.2 |
| PZ3 | Av. | 13.2 | 7.3 | 861 | 300.0 | 68.7 | 62.8 | 3.2 | 0.0 | 0.1 | 0.2 | 22.8 | 94.3 | 29.5 | 4.5 | 0.1 | 0.0 | −50.8 | −7.4 |
| | Min. | 10.3 | 7.0 | 804 | 175.0 | 62.1 | 56.9 | 0.1 | 0.0 | 0.0 | 0.1 | 21.4 | 48.8 | 26.2 | 3.9 | 0.0 | 0.0 | −51.8 | −7.7 |
| | Max. | 17.8 | 7.7 | 1180 | 343.0 | 77.0 | 71.5 | 17.1 | 0.1 | 0.2 | 0.3 | 26.1 | 103.2 | 38.5 | 11.0 | 0.5 | 0.0 | −50.0 | −7.1 |
| | SD | 2.0 | 0.2 | 63 | 25.8 | 3.3 | 2.7 | 4.4 | 0.0 | 0.0 | 0.0 | 0.9 | 11.3 | 1.8 | 1.2 | 0.1 | 0.0 | 0.5 | 0.1 |
| PZ4 | Av. | 13.3 | 7.2 | 782 | 275.1 | 51.3 | 57.0 | 12.3 | 0.0 | 0.1 | 0.2 | 18.0 | 81.8 | 32.5 | 5.0 | 0.1 | 0.0 | −51.4 | −7.6 |
| | Min. | 10.5 | 7.0 | 425 | 157.0 | 28.3 | 23.8 | 3.4 | 0.0 | 0.0 | 0.1 | 12.3 | 32.0 | 15.8 | 3.4 | 0.0 | 0.0 | −53.2 | −8.0 |
| | Max. | 17.6 | 7.6 | 1147 | 330.0 | 62.9 | 69.2 | 23.7 | 0.0 | 0.2 | 0.4 | 24.6 | 99.7 | 47.1 | 7.0 | 0.3 | 0.0 | −50.0 | −7.4 |
| | SD | 1.9 | 0.2 | 99 | 36.0 | 6.1 | 7.5 | 4.6 | 0.0 | 0.1 | 0.1 | 1.9 | 15.4 | 4.3 | 0.5 | 0.1 | 0.0 | 0.7 | 0.1 |
| PZ5 | Av. | 12.9 | 7.3 | 938 | 335.9 | 68.2 | 76.1 | 4.7 | 0.0 | 0.1 | 0.2 | 20.0 | 110.6 | 33.7 | 6.9 | 0.1 | 0.0 | −53.3 | −7.9 |
| | Min. | 10.2 | 7.0 | 530 | 183.0 | 44.4 | 52.6 | 0.1 | 0.0 | 0.0 | 0.1 | 12.7 | 42.1 | 21.7 | 3.9 | 0.0 | 0.0 | −55.6 | −8.2 |
| | Max. | 17.6 | 7.7 | 1069 | 397.0 | 80.6 | 90.7 | 15.5 | 0.1 | 0.3 | 0.4 | 22.0 | 129.8 | 42.6 | 13.3 | 0.3 | 0.0 | −49.2 | −7.5 |
| | SD | 1.8 | 0.2 | 80 | 45.4 | 7.4 | 10.9 | 3.7 | 0.0 | 0.0 | 0.1 | 1.5 | 20.7 | 3.1 | 1.3 | 0.1 | 0.0 | 1.0 | 0.1 |
| PZ6 | Av. | 11.8 | 7.4 | 1342 | 410.9 | 124.6 | 194.2 | 4.0 | 0.0 | 0.1 | 0.4 | 43.4 | 157.4 | 49.2 | 11.7 | 0.1 | 0.0 | −51.9 | −7.6 |
| | Min. | 8.1 | 7.1 | 1026 | 170.0 | 54.5 | 89.4 | 1.1 | 0.0 | 0.0 | 0.1 | 23.6 | 32.4 | 27.8 | 1.7 | 0.0 | 0.0 | −53.0 | −7.8 |
| | Max. | 15.3 | 7.6 | 3010 | 705.0 | 477.5 | 635.3 | 7.7 | 0.1 | 0.5 | 0.9 | 140.2 | 309.5 | 158.4 | 21.8 | 0.3 | 0.0 | −49.1 | −7.2 |
| | SD | 1.6 | 0.1 | 544 | 95.2 | 128.3 | 164.5 | 1.8 | 0.0 | 0.1 | 0.2 | 35.0 | 54.8 | 37.2 | 4.7 | 0.1 | 0.0 | 1.0 | 0.1 |

deposits (from silts to gravels; Teles et al., 2004; Ounaïes et al., 2013; Sarris et al., 2018). These 3D heterogeneities lead to variations in water flows distribution within the aquifer.

To summarize, hydrodynamic data highlight that during LF, Auzon Oxbow is supplied by GW. During HF, an inversion of the hydraulic gradient is recorded and Auzon Oxbow contributes to the recharge of GW. RB is entirely concerned by this recharge while only the oxbow closest borehole (PZ4) is affected in the LB (Fig. 3b). The important time delay observed between surface water flood peaks and GW recharge at PZ3, PZ5 and PZ6 (from 24 to 26 h) indicates that LB GW is mainly recharged by the southern GW system.

### 4.1.2. Physico-chemical data

For the 21 sample sites, physico-chemical parameters measurements (water temperature – T; pH; electrical conductivity – EC) as well as ions concentrations and water stable isotopes determinations are presented in Table 1 with average (arithmetic means), minimum, maximum and standard deviation values. EC vs T data of the entire SOAHAL observatory are reported in Fig. 4a while EC time-series of Auzon Oxbow DZ (B2bis), IZ (B4), UZ (B7) and of each end-member are quoted in Fig. 4b: Allier River, PZ1 (RB GW), PZ3-PZ4 (LB GW with an increasing distance to the Auzon Oxbow from PZ4 to PZ3).

The pH values are comprised between 6.5 and 8.8 (Table 1), which is consistent with natural water pH usually ranging from 6.5 to 9.5. The more neutral values have been recorded in GW and are assumed to be due to the buffering capacity of soils. EC and T values were the most interesting physico-chemical parameters to differentiate water end-members (Fig. 4):

- Allier River EC is the lowest one within the study site (110 ± 17 $\mu S.cm^{-1}$; Table 1), without any significant variations during the year (Fig. 4b). On the contrary T experiences high amplitudes (from 0.9 to 21.8 °C; Table 1) as an impact of air temperature annual variation.
- PZ1 and PZ2 show the lowest EC values of the boreholes (with 290 and 491 $\mu S.cm^{-1}$ respectively; Table 1). EC annual variations are

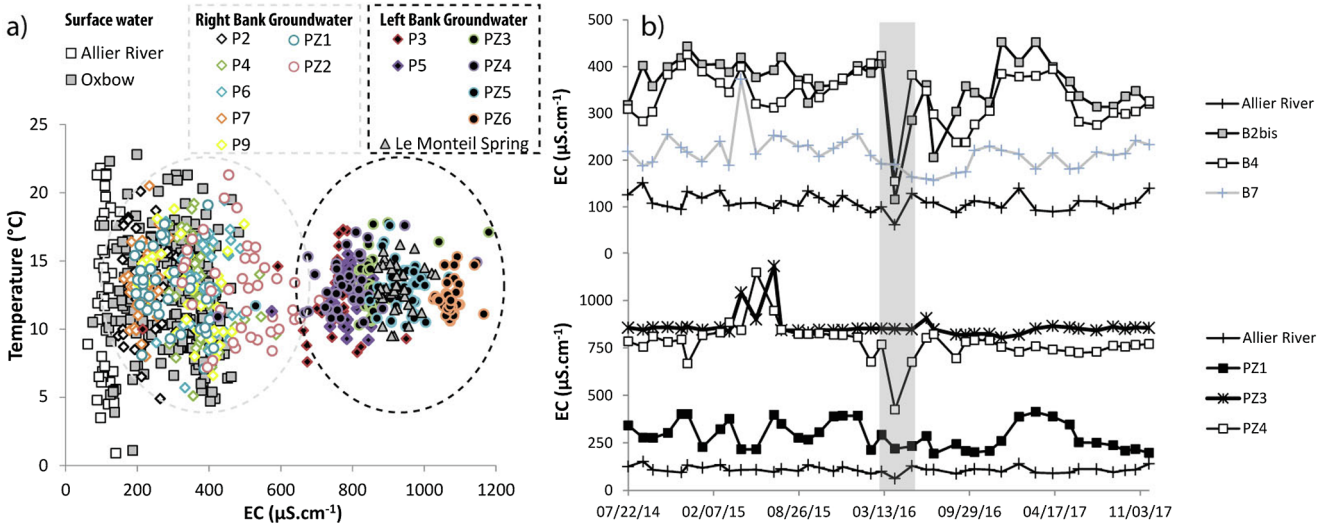


**Fig. 4.** a) EC vs Water T for all the dataset; b) Variations of EC of Allier River, B2bis (Auzon Oxbow DZ), B4 (Auzon Oxbow IZ), and B7 (Auzon Oxbow UZ), PZ1 (RB GW), PZ3-PZ4 (LB GW); the grey area highlights the decrease of EC during the April 2016 campaign in the Auzon Oxbow and PZ4.

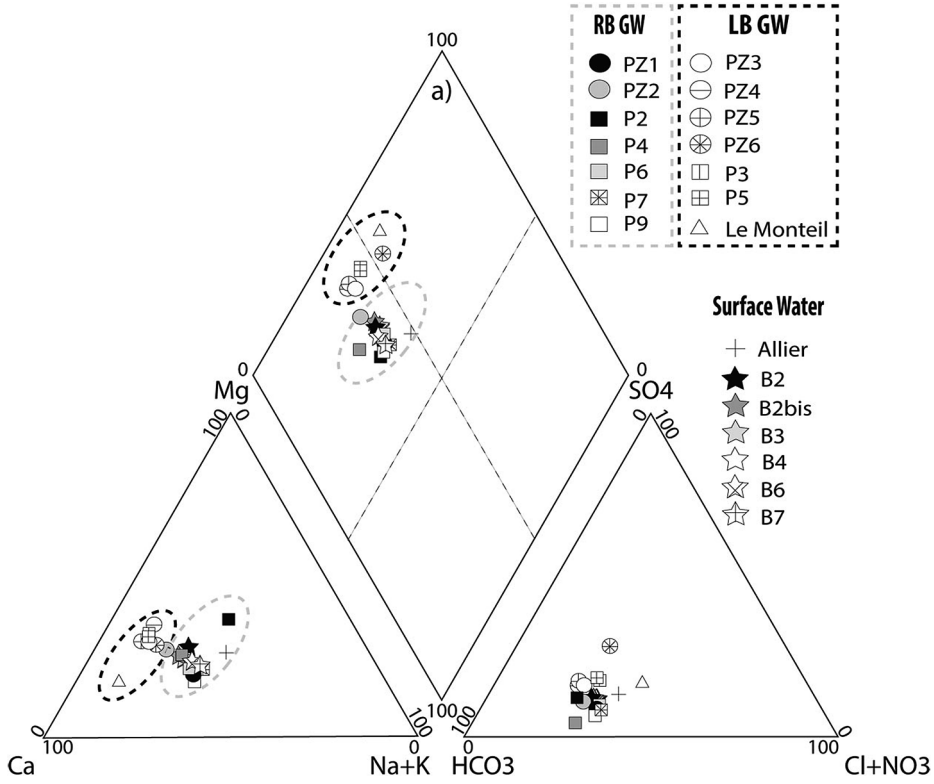


**Fig. 5.** Chemical water types of the 21 sampling sites given by a Piper's diagram established from data in $mg.l^{-1}$.

relatively low (Fig. 4b) while T amplitudes can reach more than 12 °C (Table 1). The RB (P2, P4, P6, and P9) and LB (P7) near-surface piezometers (Fig. 1c) also present low EC values and high T amplitudes (Fig. 4a and Table 1).

- PZ3 to PZ6 are characterized by the highest EC values (mean value of the four boreholes: 981 $\mu S.cm^{-1}$) while T experienced the smaller variations (around 7 °C; Table 1). EC time-series show a quite stable signal with no clearly identified seasonal variations (Fig. 4b). P3 and P5, the two remaining LB near-surface piezometers (Fig. 1c) present similar EC and T patterns (Fig. 4a and Table 1).
- Le Monteil spring shows a high EC value (925 $\mu S.cm^{-1}$, Table 1) and low amplitude of T (6.7 °C; Table 1) which is consistent with the LB GW (Fig. 4a).

#### 4.1.3. Hydrochemical data

Hydrochemical data of Table 1 have been plotted on a Piper diagram (Fig. 5) in order to define the geochemical water-types of each end-member. Water types are distributed between two groups with a noticeable difference in the cations content. The first group has a Ca-Na/$HCO_3$ type and includes Allier River, PZ1-PZ2 (RB GW), P2-P4-P6-P9 (RB near-surface piezometers), P7 (LB near-surface piezometer) and then the second group presents a Ca/$HCO_3$ signature and corresponds to PZ3 to PZ6 (LB GW), P3 and P5 (the two remaining LB near-surface piezometers) and Le Monteil Spring. Then, the GW signal shows a clear distribution between RB and LB. RB GW are predominantly supplied by Allier River whereas LB GW chemical facies is consistent with the one of the plateau aquifer (Le Monteil). This is in agreement with hydrodynamic data. P7 can be quoted as an exception to this RB/LB GW distribution, as this LB near-surface piezometer presents physico-chemical and geochemical characteristics close to the RB GW ones.

Chemical difference between Allier River (as well as RB GW) and LB GW is due to the geological composition of the watershed. Actually, the Ca-Na/$HCO_3$ water type of the Allier River can be related to the volcano-metamorphic basement: upstream of the study site, the Allier River incised the basement while downwards, the riverbed widens within the Brioude basin where an enrichment in calcareous nodules between Vieille Brioude and the study site has been documented (Lasnier and Marchand, 1982). Carbonate dissolution occurrences are reported in the Allier River and the shallow GW associated (Négrel et al., 2004). Sodium minerals, subjects to weathering, are reported as common in the Allier terraces, as augite, green and brown hornblende and nepheline (Rudel, 1963; Pastre, 1986; Veldkamp and Jongmans, 1990), which explain the Na-enriched signature of the Allier River and so that of the RB GW. The Ca/$HCO_3$ water type of LB GW has been already described by several authors (Négrel et al., 2004; Vanderhaeghe and Prognon, 2012; Mohammed et al., 2014) and corresponds to many alluvial aquifers in France (Roux, 2006) and over the world (Chkirbene et al., 2009; Andrade and Stigter, 2011; Huang et al., 2014). Indeed, because the mineral phases that composed alluvial aquifers do not generally impose a very marked geochemical type and because of short residence times within the aquifer, alluvial GW presents frequently a Ca/$HCO_3$ water type (Roux, 2006).

### 4.2. Auzon Oxbow as a result of the mixing between end-members

#### 4.2.1. General features of Auzon Oxbow chemistry

In a first approximation, taking into account their origin, perifluvial oxbows and main stream are supposed to have a similar chemical composition (Négrel et al., 2003). However, despite its still active connection with the Allier River, the Auzon Oxbow presents a mean EC value (300 $\mu S.cm^{-1}$) higher than Allier River one (110 $\mu S.cm^{-1}$) but lower than GW (784 $\mu S.cm^{-1}$ in mean for observation boreholes of both banks). This indicates that the Auzon Oxbow water results from a mixing between the low concentration water of the Allier River and the more concentrated one of GW, whatever the bank (Table 1, Fig. 4). Fig. 6 confirms this trend and highlights a clear evolution of the Auzon Oxbow between a Na-pole characterized by Allier River and a more calcic end member delineated by LB GW. RB GW water type is close to the Auzon Oxbow one and seems to result also from the mixing between Allier River and LB GW. The proximity of LB GW and Le Monteil spring

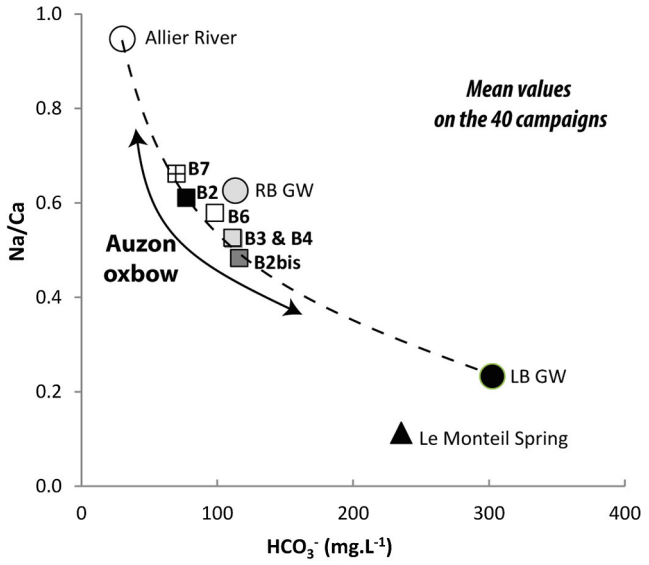


**Fig. 6.** $HCO_3^-$ vs $Na^+/Ca^{2+}$ ($mg.l^{-1}$) for Allier River, RB GW (mean of P2, P4, P6, P7, P9, PZ1 and PZ2), LB GW (mean of P3, P5, PZ3, PZ4, PZ5 and PZ6), Auzon Oxbow (B2 to B7) and Le Monteil Spring. The dashed line is an indicative mixing line between Allier River and LB GW end-members which explain the Auzon Oxbow signatures.

confirms the contribution of the plateau aquifer to the alluvial GW. This general feature is however not constant within the hydrological cycle: records of April 2016 (highlighted by the grey area of Fig. 4b) show a decrease of Auzon Oxbow EC which reaches the value of Allier River. This specific period corresponds to one of the major floods that have affected the Allier River during the study, with a discharge flow of 150 $m^3.s^{-1}$ registered on the 04/06/16 (Fig. 2d). During this period, the Allier River penetrated further into the Auzon Oxbow. This surface water arrival, characterized by a low concentration, affected the Auzon Oxbow up to B6, B7 showing constant EC. This was a short-time process since Auzon Oxbow recovered its pre-flood concentration the month after (Fig. 4b), indicating that the oxbow restitutes quickly to the main stream what it absorbs during flood. This time-constrain phenomenon has already been quoted for oxbows by Carrel and Juget (1987) for the Morte du Sauget, one of the Rhône oxbows and for oxbows of Ain River (Le Coz, 2003). PZ4 records also an EC decrease in April 2016, in accordance with the inversion of the hydraulic gradient showed in HF piezometric map (Fig. 3b).

#### 4.2.2. Identification of punctual arrivals of GW within Auzon Oxbow

To precise the downstream-upstream evolution within the Auzon Oxbow, a fine cartography of EC has been performed on the 11/23/2017, during a low flow stage (Allier River daily discharge: 6.7 $m^3.s^{-1}$). Fig. 7 presents the results of this campaign and puts in evidence a difference between the upstream zone characterized by low EC values, mainly in the range 0–250 $\mu S.cm^{-1}$, and IZ and DZ parts of the Auzon Oxbow with values comprised between 250 and 400 $\mu S.cm^{-1}$. This general pattern is disturbed by local arrivals of water. A high EC is observed along the downstream zone left bank (point 103 = 735 $\mu S.cm^{-1}$; Fig. 7) and testifies for a high concentration groundwater arrival. On the contrary, the whole upstream part is characterized by low EC in accordance with low concentration water incomes, some of which were identified as coming from the bed of the oxbow. Points 3 (as an example of the latter) and 103 have been sampled for ions analyses.

Physico-chemical parameters and ions concentrations of samples acquired on the 11/23–24/2017 for the points 3, 103 and the 21 followed sites are reported in Table 2. Results show that:

- Point 103 presents a $Ca/HCO_3$ signature pretty close to that of LB GW (Fig. 8) and especially PZ4 (Table 2, Fig. 8). PZ4 shows higher $NO_3^-$ (13.1 $mg.l^{-1}$) probably due to a contamination of alluvial GW, but not transmitted or degraded before the transfer LB GW to Auzon Oxbow.
- The low concentration water arrival located at the UZ end of the oxbow (Point 3) presents a $Ca\text{-}Na/HCO_3$ water type similar to Allier River one (Table 2, Fig. 8). This is in accordance with an upstream supply by the Allier River. The water arrival of Point 3 was coming from the bed of the oxbow which indicates that this supply is realized through underground inflows. The location of these low concentration water arrivals directly close to the paleochannel visible in the landscape, suggests that an old and deeper channel connects Auzon Oxbow to Allier River. The potential recharge by underground paleochannels, because of their high hydraulic conductivity, has already been observed (Rathore et al., 2010; Babka et al., 2011).

Therefore, to verify the present hypothesis, an ERT sounding has been performed on the 02/21/2018 (high flow period, Allier River daily discharge = 57.3 $m^3.s^{-1}$, see part 3.3). The location of the profile is indicated in Fig. 1c. Oriented SSE-NNW, the profile was designed perpendicularly to the visible paleochannel and close to the upstream end of the Auzon Oxbow. Indeed, electrical resistivity sounding has already been used to investigate subsurface paleochannel geometry, architecture and hydrodynamic (Sinha et al., 2013) as well as fresh GW discharge through a paleochannel (Kolker et al., 2013). The resulting ERT profile indicates a general decrease of the electrical resistivity with depth (Fig. 9). Two main zones can however be observed. In the first one, from surface to 8–10 m depth, resistivity varies laterally. The southern part of the profile, along with the 48 first lateral meters on Fig. 9, presents a relatively low resistivity ($\rho$ = 150–350 $\Omega.m^{-1}$) compared to the rest of the section ($\rho$ > 600 $\Omega.m^{-1}$). It can be interpreted as a sand formation saturated with freshwater (Sinha et al., 2013). This is consistent with the presence of the paleochannel of the Allier River (Fig. 1c), which higher porosity induces lower resistivity (Archie, 1942). In addition, there is lateral resistivity change within the paleochannel which most likely reflects the progressive filling of the system and a potential connection to the river (blue circle on Fig. 9). The second zone starts below 10 m depth with low resistivity values and corresponds to the Oligocene marl substratum (Lasnier and Marchand, 1982; Korobova et al., 1997).

This paleochannel supplies the Auzon Oxbow with low concentration water and explains the low EC and the water types observed in the upstream part of the Auzon Oxbow and in the near-surface piezometer P7 (Fig. 1c). The repartition of Auzon Oxbow points along the mixing line of the Fig. 6, with B7 closer to the Allier River end-member than B2 is thus explained. For information, a simple estimation of contribution percentages of Allier River and LB GW to the oxbow (at its different sampling locations) can therefore been deduced from the Fig. 6 data. Indeed, considering that the chemical characteristics of the Allier River end-member point (30.2 $mg.l^{-1}$ of $HCO_3^-$ and a Na/Ca ratio of 0.95) represent 100% of contribution from the main stream and that those of LB GW (302.6 $mg.l^{-1}$ of $HCO_3^-$ and a Na/Ca ratio of 0.23) represent 0%, it is easy to deduce the contributions of those end-member to the oxbow at the different sampling sites. So, it was logically estimated that B2, the closest location to the confluence and B7, the closest location to the paleochannel arrival, were mostly and equally fed by the Allier River with respectively 63 and 64% of contribution. The rest of the oxbow would be, according to these strictly indicative estimates, as much fed by the river as by the alluvial groundwater (49% of Allier River contribution for B3, 50% for B4 and 51% for B2bis and B6). Those estimates would imply that alluvial groundwater contributions to the Auzon oxbow are not negligible and that, in terms of contribution share, the river contributes as much by the confluence as by the upstream paleochannel to the oxbow water supply.

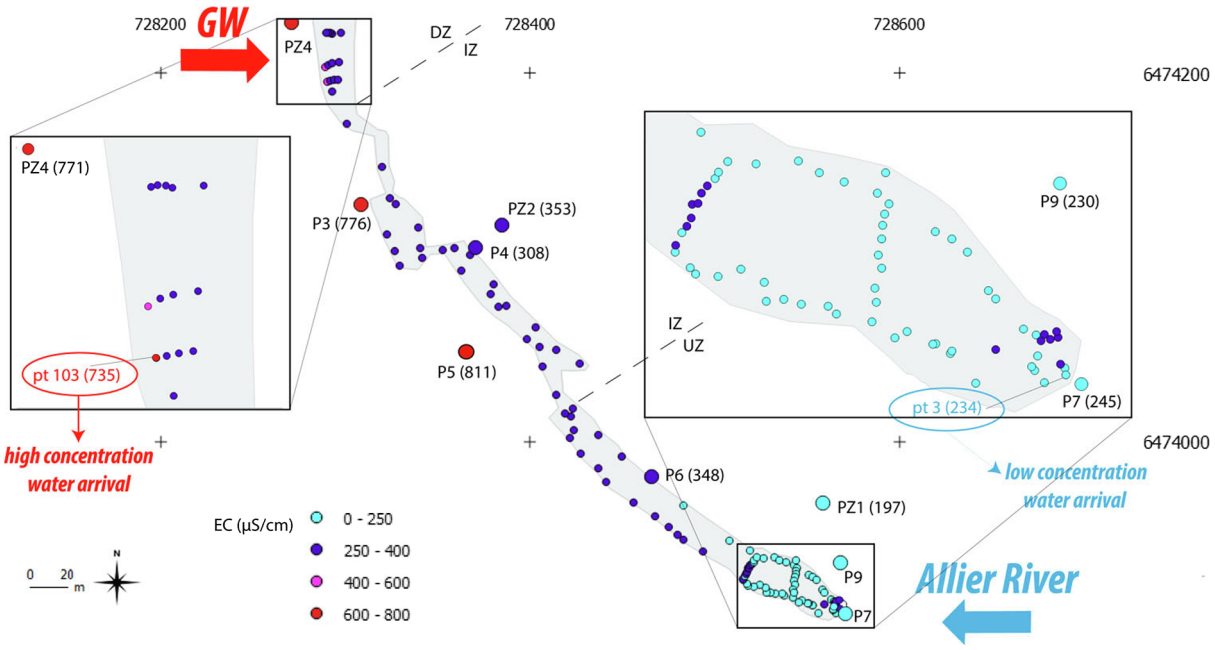


**Fig. 7.** Cartography of EC performed on the 11/23/2017.

*4.2.3. Use of $\delta^2H$ and $\delta^{18}O$ of the water molecule for temporal insight*

The $^2H$-$^{18}O$ stable isotopes of the water molecule constitute one of the best water tracer since it provides information about water origins as well as water mixing processes through the hydrological cycle (Fontes, 1980; Clark and Fritz, 1997; Kendall and McDonnell, 1999). For the study of wetlands, they allow approaching their functioning (Hunt et al., 1998; Clay et al., 2004) and more peculiarly to characterize the isotopic content of the different supplying sources or the Auzon Oxbow (Babka et al., 2011) according to the temperature-, amount-, altitudinal- and continental-effects (Rozanski et al., 2001).

For coherent interpretations, data from April to November 2017, period of the concomitant investigation of all sites, have been selected among the database. Allier River (−8.0 $\delta^{18}O$‰, −52.0 $\delta^2H$‰) and RB GW (−8.1 $\delta^{18}O$‰, −53.2 $\delta^2H$‰) present the most depleted isotopic content. The LB GW (−7.7 $\delta^{18}O$‰, −51.5 $\delta^2H$‰) and Le Monteil spring (−7.3 $\delta^{18}O$‰, −50.0 $\delta^2H$‰) are characterized by more enriched signatures. As previously referred by Négrel et al. (2003) and by Mohammed et al. (2014), Allier River displays a clear seasonal variation (Fig. 10a) with depleted values during winter and more generally during HF period (around −8.5 $\delta^{18}O$‰) than for summer (around −7.5‰), mainly due to the temperature effect on precipitation. Fig. 10b shows $\delta^2H_{VSMOW}$ (‰) vs $\delta^{18}O_{VSMOW}$ (‰) means for Auzon Oxbow sampling sites and its end-members. Taking into account the high variability of the Allier River data, all the measurements have been plotted individually. Precipitation is represented by the Global Meteoric Water Line (GMWL) of Craig (1961), and more regionally by the Local

**Table 2**
Physico-chemical parameters and ions concentrations data for the 11/23–11/24/2017 campaign.

| Sample ID | T | pH | EC | $HCO_3^-$ | $Cl^-$ | $SO_4^{2-}$ | $NO_3^-$ | $NO_2^-$ | $PO_4^{3-}$ | $F^-$ | $Na^+$ | $Ca^{2+}$ | $Mg^{2+}$ | $K^+$ | $NH_4^+$ | $Li^+$ |
|---|---|---|---|---|---|---|---|---|---|---|---|---|---|---|---|---|
| | (°C) | | ($\mu S.cm^{-1}$) | ($mg.l^{-1}$) | | | | | | | | | | | | |
| Allier | 5.6 | 7.5 | 140 | 39.0 | 14.7 | 7.9 | 2.3 | 0.0 | 0.09 | 0.1 | 9.6 | 10.4 | 4.3 | 1.9 | 0.0 | 0.0 |
| B2 | 6.7 | 7.4 | 218 | 62.0 | 20.3 | 11.8 | 1.9 | 0.0 | 0.11 | 0.1 | 11.5 | 19.4 | 6.8 | 2.4 | 0.0 | 0.0 |
| B2bis | 8.7 | 7.1 | 320 | 108.0 | 29.4 | 15.5 | 0.7 | 0.0 | 0.11 | 0.2 | 15.4 | 30.6 | 9.0 | 3.3 | 0.0 | 0.0 |
| B3 | 8.5 | 7.0 | 314 | 113.0 | 29.3 | 14.7 | 0.6 | 0.0 | 0.08 | 0.2 | 15.7 | 29.9 | 8.7 | 3.5 | 0.0 | 0.0 |
| B4 | 9.1 | 7.2 | 326 | 105.0 | 30.1 | 14.3 | 1.0 | 0.0 | 0.12 | 0.2 | 16.2 | 31.1 | 8.9 | 3.6 | 0.0 | 0.0 |
| B6 | 10.3 | 7.0 | 243 | 81.0 | 22.9 | 11.6 | 1.4 | 0.0 | 0.11 | 0.2 | 12.8 | 22.4 | 6.9 | 2.8 | 0.0 | 0.0 |
| B7 | 12.7 | 7.0 | 233 | 81.0 | 26.1 | 12.6 | 1.0 | 0.0 | 0.14 | 0.1 | 14.4 | 23.1 | 6.4 | 2.9 | 0.0 | 0.0 |
| pt3 | 12.8 | x | 234 | 62.0 | 23.0 | 12.1 | 2.2 | 0.0 | 0.08 | 0.2 | 13.4 | 20.4 | 6.0 | 2.7 | 0.0 | 0.0 |
| Monteil | 12.6 | 7.1 | 872 | 226.0 | 57.5 | 64.3 | 95.0 | 0.1 | 0.15 | 0.5 | 12.5 | 123.8 | 17.1 | 11.0 | 0.0 | 0.0 |
| P2 | 10.4 | 7.0 | 269 | 117.0 | 13.8 | 8.9 | 0.1 | 0.0 | 0.05 | 0.2 | 12.2 | 19.4 | 11.3 | 2.3 | 0.0 | 0.0 |
| P3 | 11.6 | 7.1 | 776 | 243.0 | 60.4 | 73.4 | 27.2 | 0.0 | 0.14 | 0.3 | 17.7 | 89.4 | 29.0 | 4.4 | 0.1 | 0.0 |
| P4 | 7.9 | 7.0 | 308 | 111.0 | 29.0 | 3.5 | 0.1 | 0.0 | 0.07 | 0.2 | 14.1 | 28.4 | 8.1 | 2.5 | 0.9 | 0.0 |
| P5 | 11.9 | 7.2 | 811 | 265.0 | 65.9 | 66.4 | 25.5 | 0.0 | 0.09 | 0.3 | 20.5 | 95.3 | 29.1 | 3.2 | 0.1 | 0.0 |
| P6 | 10.4 | 6.9 | 348 | 127.0 | 28.7 | 14.9 | 1.9 | 0.0 | 0.03 | 0.3 | 15.8 | 35.3 | 9.4 | 3.7 | 0.0 | 0.0 |
| P7 | 12.5 | 6.6 | 245 | 74.0 | 25.6 | 10.8 | 1.2 | 0.0 | 0.08 | 0.1 | 14.6 | 22.9 | 6.6 | 2.6 | 0.0 | 0.0 |
| P9 | 11.4 | 6.7 | 230 | 78.0 | 20.4 | 9.2 | 0.2 | 0.0 | 0.05 | 0.2 | 12.4 | 22.9 | 5.0 | 2.8 | 0.0 | 0.0 |
| PZ1 | 12.6 | 7.0 | 197 | 82.0 | 16.0 | 6.4 | 0.1 | 0.0 | 0.08 | 0.2 | 11.1 | 19.0 | 4.5 | 2.6 | 0.0 | 0.0 |
| PZ2 | 11.8 | 7.3 | 353 | 136.0 | 28.9 | 7.0 | 0.2 | 0.0 | 0.06 | 0.2 | 14.5 | 32.8 | 9.5 | 2.9 | 0.4 | 0.0 |
| PZ3 | 13.0 | 7.1 | 855 | 308.0 | 69.9 | 61.5 | 3.0 | 0.0 | 0.12 | 0.2 | 22.5 | 98.0 | 29.4 | 4.2 | 0.1 | 0.0 |
| PZ4 | 13.2 | 7.2 | 771 | 279.0 | 52.4 | 61.5 | 13.1 | 0.0 | 0.09 | 0.3 | 17.4 | 85.9 | 32.1 | 5.1 | 0.0 | 0.0 |
| pt103 | 11.2 | x | 735 | 282.0 | 56.6 | 60.9 | 0.1 | 0.0 | 0.21 | 0.3 | 17.8 | 87.9 | 31.0 | 5.1 | 0.2 | 0.0 |
| PZ5 | 13.2 | 7.3 | 1002 | 374.0 | 70.2 | 85.8 | 2.1 | 0.0 | 0.18 | 0.3 | 21.3 | 129.0 | 34.9 | 7.6 | 0.1 | 0.0 |
| PZ6 | 12.1 | 7.3 | 1074 | 405.0 | 62.2 | 107.6 | 6.1 | 0.0 | 0.12 | 0.4 | 26.1 | 150.4 | 31.3 | 13.6 | 0.1 | 0.0 |

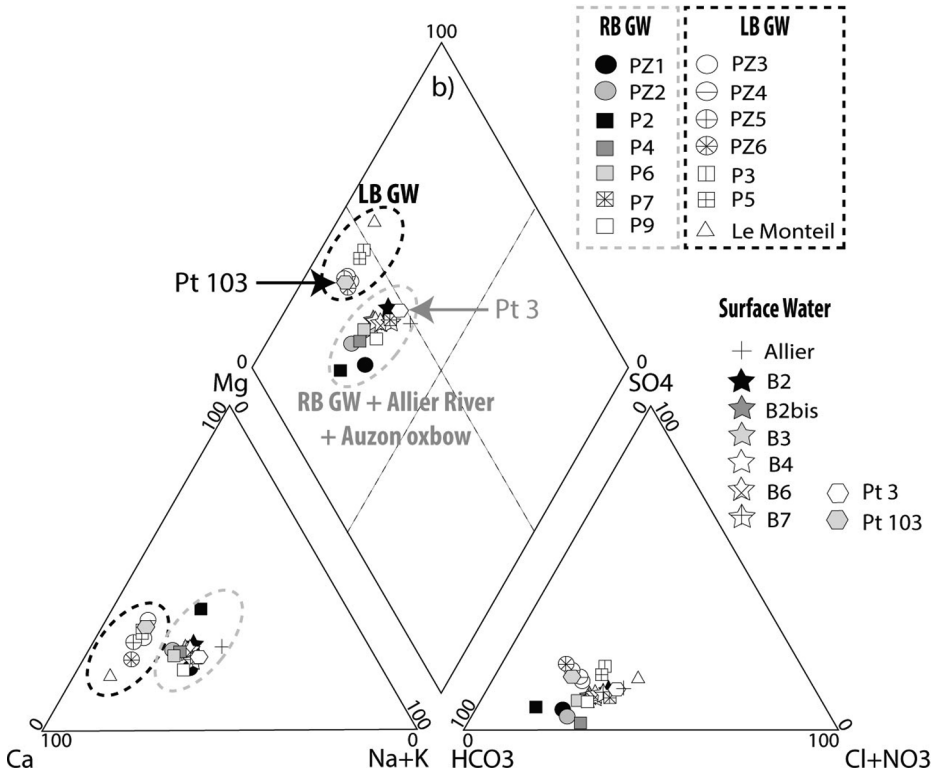


**Fig. 8.** Piper's diagram established from data in mg.l$^{-1}$ of the 21 sampling sites and of the two water arrivals (Pt 3 and 103) analyzed for the 11/23–24/17 campaign.

Meteoric Water Line (LMWL) proposed by Petelet-Giraud et al. (2005) with a local average of $\delta^2H = 8^* \delta^{18}O + 13.7‰$ and low altitude rainfalls of Cournon (03°13′33″E/45°44′54″N; elevation: 327 m; period 2013–2016; AUVERWATCH Database, 2018; Celle-Jeanton, 2017). All data follow a trend line between LMWL and local precipitation of Cournon rainfall, the more depleted signal is characterized by the samples of Allier River during HF (−8.5 $\delta^{18}O‰$, −55.0 $\delta^2H‰$) while the more enriched by the Allier River LF ones (−7.4 $\delta^{18}O‰$, −49.1 $\delta^2H‰$), LB GW (−7.7 $\delta^{18}O‰$, −51.5 $\delta^2H‰$) and Le Monteil spring (−7.3 $\delta^{18}O‰$, −50.0 $\delta^2H‰$). Allier River HF data follow the LMWL and are representative of the colder and higher altitude precipitation. The more enriched and evaporated signal of Allier River LF is explained by low altitude precipitation (summer local storms) and/or local GW supply. This is consistent with the previous conclusions based on hydrodynamic data that showed relationships between low flow surface water and groundwater, with more enriched GW during summer, due to evaporation process (Geyh and Mook, 2000; Mohammed et al., 2014). Auzon Oxbow isotopic data are well plotted along a mixing line between Allier River HF and isotopically enriched waters. Auzon Oxbow DZ (B2 and B2bis) presents the more enriched and evaporated signal close to that of the LB GW; the heavy isotopes content globally decreases up to the UZ (B7; Fig. 10b). On a temporal scale, evolution of isotopic data in the Auzon Oxbow tends to homogenize and the 3 identified zones DZ (B2bis), IZ (B4) and UZ (B7) present, in winter period, the same isotopic content (Fig. 10a). This behavior is partly explained by previous observations: DZ is subject to a double supply through its connection to the Allier River at the confluence and LB GW inputs (Point 103). The later explains the more enrich isotopes contents and its important variations through time. B7 has been shown to be supplied by Allier River that inflows to the Auzon Oxbow through the subsurface paleochannel. However, B7 presents a behavior completely different from the one of Allier River and isotopic values of B7 match only the Allier River ones during winter high flow period (Fig. 10a). This observation provides precision about the recharge of the Auzon Oxbow from the paleochannel that occurs only seasonally, during HF periods, as for the RB GW. Indeed, according to the hydrodynamic monitoring, the RB GW recharge through inversion of the hydraulic gradient during HF which is also in agreement with the depleted isotopic values observed for RB GW.

### 4.3. Conceptual model of the Auzon Oxbow

The multidisciplinary analysis between hydrodynamic, geochemical and isotopic approaches carried out at the dense SOAHAL Observatory allows establishing a reliable conceptual model of the hydrodynamical functioning of the Auzon Oxbow (Fig. 11). As expected for that kind of

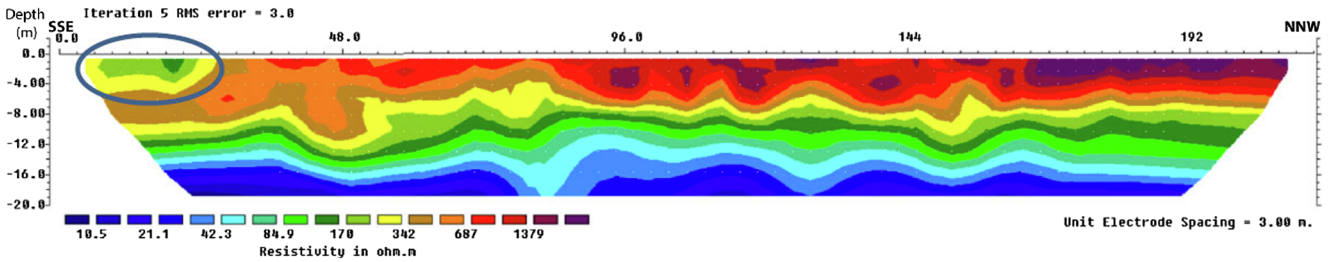


**Fig. 9.** ERT profile crossing the active paleochannel (blue circle) upstream from the Auzon Oxbow (orientation SSE-NNW). (For interpretation of the references to colour in this figure legend, the reader is referred to the web version of this article.)

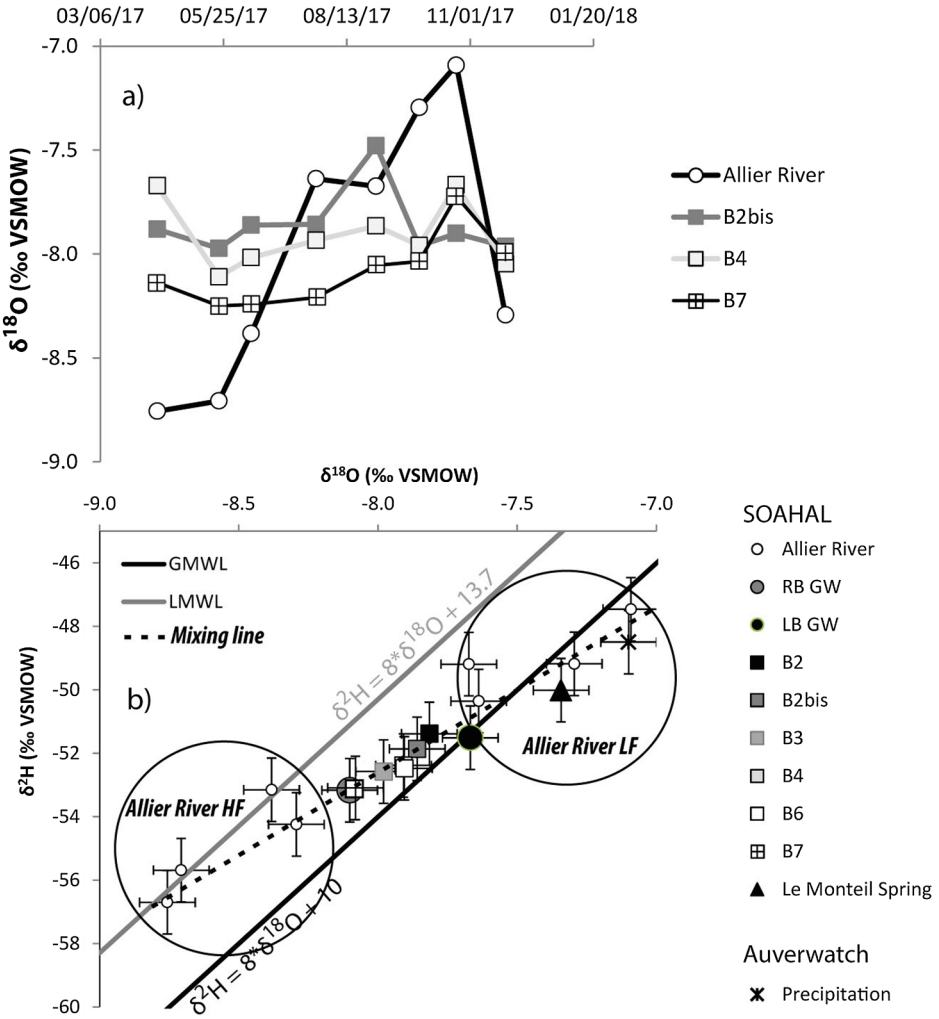


**Fig. 10.** a) $\delta^{18}O$ time-series for Allier River and Auzon Oxbow (DZ: B2bis; IZ: B4; UZ: B7) from April to November 2017; b) $\delta^{2}H$ and $\delta^{18}O$ signatures for Allier River, RB GW (mean of P2, P4, P6, P7, P9, PZ1 and PZ2), LB GW (mean of P3, P5, PZ3, PZ4, PZ5 and PZ6), Auzon Oxbow (B2 to B7) and Le Monteil spring. Local Meteoric Water Line (LMWL: $\delta^{2}H = 8*\delta^{18}O + 13.7$‰ by Petelet-Giraud et al. (2005)) and Global Meteoric Water Line (GMWL: $\delta^{2}H = 8*\delta^{18}O + 10$‰ by Craig (1961)) are also shown for comparison.

perifluvial environments (Rollet et al., 2005), interactions between the oxbow and both the main stream and the alluvial aquifer were identified. Since the Auzon Oxbow is disconnected from the main stream in its upstream end for the last 30 years, the Allier River supplies the oxbow generally through the downstream confluence (surface water flows on Fig. 11). However, during major flood events the main stream can submerge the right bank and then supply the entire oxbow area. Geochemical data show another interaction between the Allier River and the Auzon Oxbow, through the upstream underground paleochannel, recognized both via geochemical analysis and geophysical investigations. A detailed isotopic analysis has shown that this Auzon Oxbow area has a similar isotopic signature than Allier River during high flow periods only. This observation implies that the paleochannel is active from November to June only. This is in agreement with the results of hydrodynamic and geochemical approaches which identified existing pathways from surface water to alluvial groundwater during the same periods (high flow GW flows on Fig. 11).

The coupling approach also testifies for a supply of the oxbow by the alluvial groundwater, this especially affects the water composition in its downstream part. As this part of the oxbow is the site of its confluence to the Allier River, groundwater supply could have been underestimated otherwise. That connection with the adjunct alluvial aquifer is active during low flow (Fig. 11). LB GW are mainly supplied by the southern part of alluvial aquifer and the neighboring agricultural plateau (permanent GW flows on Fig. 11), except during high floods when small gradient inversions can drive pathways from surface water to groundwater.

The active connection existing between the Auzon Oxbow and the Allier River through the underground paleochannel would not have been identified and specified without the geochemical and isotopic approaches. A standard hydrodynamic study based on their apparent geomorphological surface connection would have produced an incomplete understanding of the Auzon Oxbow hydrosystem. Besides, while studies attest for the importance of oxbow connection degree to the main stream on the water quality (Carrel and Juget, 1987; Bengen et al., 1992), it is mostly based on the type of surface connection observed between the two water bodies (oxbow isolated from the river or connected through one or two sides as Ward et al. (2002) described). Those observations indeed inform about the extent of the hydrological connection that impacts the water chemistry of oxbows (Tockner et al., 1999; Glińska-Lewczuk, 2009) especially for instance for metals contaminations (Ciazela et al., 2018). However, the present study show that consequent underground connection can also occur between the main stream and the oxbow through paleochannel as already suggested by Babka et al. (2011), increasing so their apparent connection degree and impacting the water chemistry of the oxbow. Therefore, the possibility of underground connectivity to the main stream should be further considered in oxbows hydrogeological studies. Applying

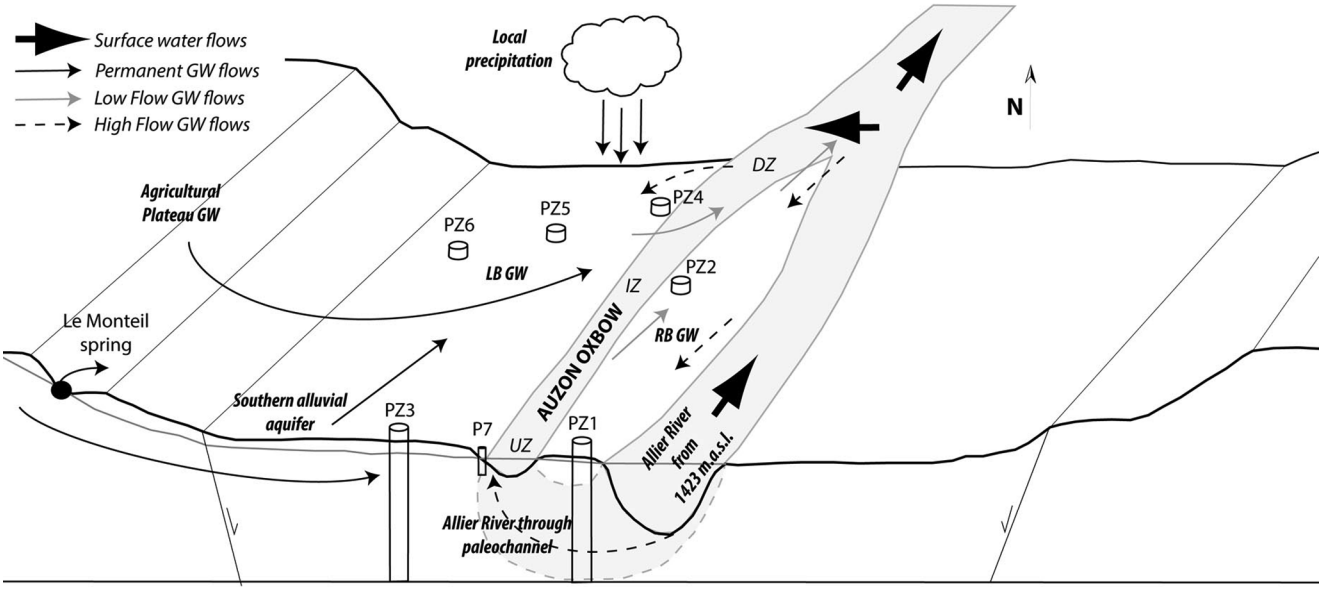


**Fig. 11.** Conceptual model of the Auzon Oxbow: identification of its interactions with the Allier River and the alluvial aquifer. The river supplies its annex by the surface connection at the downstream confluence and by an underground connection through the upstream paleochannel (which recharge during HF). The alluvial groundwater of the left bank was identified to supply the oxbow during LF especially in its downstream part.

multidisciplinary approach as the one performed on the Auzon Oxbow should so be essential to the establishment of reliable conceptual models and to their resulting management applications.

## 5. Conclusions

In a near future, wetlands like oxbows are assumed to become more and more determinant as nature-based solutions to respond to hydrological (river discharge control) and ecological (excess nutrients removal function) concerns. Therefore, the dynamic of these specific hydrosystems must be fully understood. However, the establishment of complete and useful functioning models is complicated by the different connection degrees that can have these specific wetlands with the surrounding water masses. The task is all the more difficult since it is usually undertaken through individual investigation approach which can neglect or underestimate some supply components. The objectives of the present study were so to provide effective diagnostic tools to evaluate oxbow connection degree to the main stream and to the adjunct alluvial aquifer in order to be able to establish a complete hydrodynamic description of such hydrosystems.

The Auzon Oxbow conservation is the subject of local/regional great concerns especially for the local fishing associations. In fact, hydrodynamic and hydrochemical features of Auzon Oxbow have a direct impact on its ecological functions as reproduction and refuge areas for emblematic fishes such as trouts. This study so proposed the coupling of hydrodynamic, geochemical and isotopic approaches to produce a model which can serve as a reference state for further operations of conservation and management of the Auzon Oxbow. The conceptual model thus produced attests to a greater degree of connection than expected between the Auzon Oxbow and both the main stream and the alluvial aquifer. Indeed, despite their surface upstream disconnection for the last 30 years, the study proved that Allier River supplies the oxbow through the downstream confluence and through the upstream underground paleochannel. Besides, the model attests to a non-negligible supply of the Auzon oxbow by the adjunct alluvial aquifer.

The current model can however be improved by completing the present hydrodynamic monitoring set with hydrological stations within the oxbow: one at the upstream ends of its downstream zone to compare data with the current hydrological station of the confluence; and one at the upstream end of the oxbow, close to the paleochannel water arrival. Flowrates measurements must indeed be performed in order to be able to quantify the water fluxes identified in this paper. Thus, the Auzon Oxbow role to manage flood events in the Allier River system would be evaluated. Besides, the impact of the Allier River arrival through the paleochannel on the water level of the upstream zone of the oxbow would be assessed. Furthermore, such reliable conceptual models can be used for further applications: strategic wetlands operations or water quality managements responding to environmental and/or ecological issues. Indeed, such hydrodynamic knowledges on hydrosystems constitute an essential requirement to understand the transport of polluting substances by water. The conceptual hydrodynamic scheme coupled with the contaminants observations can support the assessment of the origin(s) and fate(s) of pollutants within wetlands hydrosystems and the identification of potential remediation processes occurences. The present conceptual model of the Auzon Oxbow hydrosystem is currently used to assess the role of that wetland regarding to excess nutrients and emerging molecules dynamics.

The study here proved that coupling several investigation approaches such as hydrodynamic (surface water and groundwater levels), geochemical (physico-chemical parameters and ionic concentrations) and isotopic ($\delta^2$H-$\delta^{18}$O of the water molecule) monitorings actually efficiently supports the identification of water supply sources to the wetland through space and time. Indeed, while the hydrodynamic approach gives general informations about surface water/groundwater interactions, the geochemical and isotopic approaches complete the overview by identifying the origin of water, imaging the hydrochemistry of the oxbow and following the evolution of hydrodynamical and chemical parameters within time. Spatial and temporal disparities in the oxbow connection degree to the main stream and to the alluvial groundwater are proved to largely depend on river discharge during low and high flows. Besides, relevance of considering the degree of underground connection between the oxbow and the river was highlighted. The used of the multidisciplinary approach proposed here to image oxbows is then very promising.

## Declaration of Competing Interest

None.

## Acknowledgments

The study was funded by the European Regional Development Fund (ERDF 2014-2020) through the CPER project “Les phytosanitaires du champ à l’assiette”. The authors also thank the Auvergne-Rhône-Alpes Region for its financial support. Besides, the study was carried out in an interdisciplinary setting under the aegis of the FR Environnement. Thanks also to the farmers of the study area who authorized the observation boreholes installation on their fields.

## References

Alard, D., Bourcier, A., Bureau, F., Lefebvre, D., Mesnage, V., Poudevigne, I., 2001. Zones humides de la basse vallée de la Seine.
Amoros, C., Bornette, G., 2002. Connectivity and biocomplexity in waterbodies of riverine floodplains. Freshw. Biol. 47, 761–776. https://doi.org/10.1046/j.1365-2427.2002.00905.x.
Andrade, A.I.A.S.S., Stigter, T.Y., 2011. Hydrogeochemical controls on shallow alluvial groundwater under agricultural land: case study in central Portugal. Environ. Earth Sci. 63, 809–825. https://doi.org/10.1007/s12665-010-0752-7.
Archie, G.E., 1942. The electrical resistivity log as an aid in determining some reservoir characteristics. Trans. AIME 146, 54–62. https://doi.org/10.2118/942054-G.
AUVERWATCH Database, 2018. AUVERWATCH Database [WWW Document]. https://doi.org/10.25519/AUVERWATCH-.
Babka, B., Futó, I., Szabó, S., 2011. Clustering oxbow lakes in the Upper-Tisza region on the basis of stable isotope measurements. J. Hydrol. 410, 105–113. https://doi.org/10.1016/j.jhydrol.2011.09.026.
Banque Hydro [WWW Document], n.d. URL http://hydro.eaufrance.fr/ (accessed 2.23.18).
Bates, B.C., Kundzewicz, Z.W., Wu, S., Palutikof, J.P., 2008. IPCC Technical Paper VI, Climate Change and Water. IPCC Secretariat, Geneva, Switzerland.
Beauger, A., 2008. Impact de la capture d’un chenal fluviatile par une ancienne gravière sur la distribution des macroinvertébrés benthiques. Rev. Sci. Eau J. Water Sci. 21, 87–98. https://doi.org/10.7202/017933ar.
Beauger, A., Delcoigne, A., Voldoire, O., Serieyssol, K., Peiry, J.-L., 2015. Distribution of diatom, macrophyte and benthic macroinvertebrate communities related to spatial and environmental characteristics: the example of a cut-off meander of the river Allier (France). Cryptogam. Algol. 36, 323–355. https://doi.org/10.7872/crya/v36.iss3.2015.323.
Bengen, D., Lim, P., Belaud, A., 1992. Qualité des eaux de trois bras morts de la Garonne: variabilité spatio-temporelle = Water quality in three ancient arms of the river Garonne : spatio-temporal variability. Rev. Sci. Eau FRA Hydrol. Cont. 5, 131–156.
Bornette, G., Amoros, C., Piegay, H., Tachet, J., Hein, T., 1998. Ecological complexity of wetlands within a river landscape. Biol. Conserv. 85, 35–45. https://doi.org/10.1016/S0006-3207(97)00166-3.
Bullock, A., Acreman, M., 2003. The role of wetlands in the hydrological cycle. Hydrol. Earth Syst. Sci. Discuss. 7, 358–389.
Carrel, P.G., Juget, J., 1987. La Morte du Sauget, un ancien méandre du Rhône: bilan hydrologique et biogéochimique. Swiss J. Hydrol. 49, 102–125. https://doi.org/10.1007/BF02540384.
Celle-Jeanton, H., 2017. Projet RESEAU (AUVER-WATCH) REseau de Suivi des Eaux en AUvergne (AUVERgne WATer CHemsitry) (Rapport Final 2014-2016).
Chkirbene, A., Tsujimura, M., Cheref, A., Tanaka, T., 2009. Hydro-geochemical evolution of groundwater in an alluvial aquifer: case of Kurokawa aquifer, Tochigi prefecture, Japan. Desalination 246, 485–495. https://doi.org/10.1016/j.desal.2008.04.057.
Ciazela, J., Siepak, M., Wojtowicz, P., 2018. Tracking heavy metal contamination in a complex river-oxbow lake system: middle Odra Valley, Germany/Poland. Sci. Total Environ. 616–617, 996–1006. https://doi.org/10.1016/j.scitotenv.2017.10.219.
Clark, I., Fritz, P., 1997. Environmental Isotopes in Hydrogeology.
Clay, A., Bradley, C., Gerrard, A.J., Leng, M.J., 2004. Using stable isotopes of water to infer wetland hydrological dynamics. Hydrol. Earth Syst. Sci. 8, 1164–1173. https://doi.org/10.5194/hess-8-1164-2004.
Craig, H., 1961. Isotopic variations in meteoric waters. Science 133, 1702–1703. https://doi.org/10.1126/science.133.3465.1702.
Cunningham, W.L., Schalk, C.W., comps., 2011. Groundwater technical procedures of the U.S. Geological Survey: U.S. Geological Survey Techniques and Methods 1-A1.
Dahl, T.E., 1990. Wetlands losses in the United States, 1780’s to 1980’s. U.S. Department of the Interior, Fish and Wildlife Service, Washington D.C., pp. 13.
Dahm, C.N., Grimm, N.B., Marmonier, P., Valett, H.M., Vervier, P., 1998. Nutrient dynamics at the interface between surface waters and groundwaters. Freshw. Biol. 40, 427–451. https://doi.org/10.1046/j.1365-2427.1998.00367.x.
Davidson, N., 2014. How much wetland has the world lost? Long-term and recent trends in global wetland area. Mar. Freshw. Res. 65, 936–941. https://doi.org/10.1071/MF14173.
Fontes, J.C., 1980. Environmental isotopes in groundwater hydrology. Handb. Environ. Isot. Geochem. 1.
Fretwell, J.D., Williams, J.S., Redman, P.J., 1996. National water summary on wetland resources (USGS Numbered Series No. 2425). In: Water Supply Paper. U.S. Government Printing Office, Washington, D.C.
Gagliano, S.M., Howard, P.C., 1984. The neck cutoff oxbow lake cycle along the Lower Mississippi River, in River meandering. Am. Soc. Civ. Eng. 147–158.
Gay, A., 2015. Transfert de particules des versants aux masses d’eau sur le bassin Loire-Bretagne (thesis). Tours.
Geyh, M.A., Mook, W.G., 2000. Environmental isotopes in the hydrological cycle principles and applications Volume IV. UNESCO, Paris.
Ghosh, D., Biswas, J.K., 2017. Catch per unit efforts and impacts of gears on fish abundance in an oxbow lake ecosystem in Eastern India. Environ. Health Eng. Manage. 4, 169–175.
Gleick, P.H., 1998. Water in crisis: paths to sustainable water use. Ecol. Appl. 8, 571–579. https://doi.org/10.1890/1051-0761(1998) 008[0571:WICPTS]2.0.CO;2.
Glińska-Lewczuk, K., 2009. Water quality dynamics of oxbow lakes in young glacial landscape of NE Poland in relation to their hydrological connectivity. Ecol. Eng. 35, 25–37. https://doi.org/10.1016/j.ecoleng.2008.08.012.
Huang, Y., Zhou, Z., Wang, J., Dou, Z., Guo, Q., 2014. Spatial and temporal variability of the chemistry of the shallow groundwater in the alluvial fan area of the Luanhe river, North China. Environ. Earth Sci. 72, 5123–5137. https://doi.org/10.1007/s12665-014-3383-6.
Hudson, P.F., Heitmuller, F.T., Leitch, M.B., 2012. Hydrologic connectivity of oxbow lakes along the lower Guadalupe River, Texas: the influence of geomorphic and climatic controls on the “flood pulse concept”. J. Hydrol. 414–415, 174–183. https://doi.org/10.1016/j.jhydrol.2011.10.029.
Hulton, G., 2012. Global Costs and Benefits of Drinking-water Supply and Sanitation Interventions to Reach the MDG Target and Universal Coverage.
Hunt, R., Bullen, D., Krabbenhoft, T., Kendall, C., 1998. Using stable isotopes of water and strontium to investigate the hydrology of a natural and a constructed wetland. Ground Water 39, 271–293. https://doi.org/10.1111/j.1745-6584.1998.tb02814.x.
IAEA, 2009. Laser Spectroscopic Analysis of Liquid Water Samples for Stable Hydrogen and Oxygen Isotopes.
Jubertie, F., 2006. Les excès climatiques dans le Massif Central français : l’impact des temps forts pluviométriques et anémométriques en Auvergne (thesis). Clermont-Ferrand 2.
Kendall, C., McDonnell, J.J. (Eds.), 1999. Isotope Tracers in Catchment Hydrology. Elsevier Science, Amsterdam, New York.
Kolker, A.S., Cable, J.E., Johannesson, K.H., Allison, M.A., Inniss, L.V., 2013. Pathways and processes associated with the transport of groundwater in deltaic systems. J. Hydrol. 498, 319–334. https://doi.org/10.1016/j.jhydrol.2013.06.014.
Korobova, E., Veldkamp, A., Ketner, P., Kroonenberg, S., 1997. Element partitioning in sediment, soil and vegetation in an alluvial terrace chronosequence, Limagne rift valley, France: a landscape geochemical study. CATENA 31, 91–117. https://doi.org/10.1016/S0341-8162(97)00029-5.
Larocque, M., Biron, P.M., Buffin-Bélanger, T., Needelman, M., Cloutier, C.-A., McKenzie, J.M., 2016. Role of the geomorphic setting in controlling groundwater–surface water exchanges in riverine wetlands: a case study from two southern Québec rivers (Canada). Can. Water Resour. J. Rev. Can. Ressour. Hydr. 1–15.
Lasnier, B., Marchand, J., 1982. Brioude. Carte géologique de la France à 1 (50), 000.
Le Coz, J., 2003. Réponse hydraulique d’un bras mort au signal hydrologique de la rivière.
Loke, M.H., 2016. Tutorial: 2-D and 3-D electrical Imaging surveys. IRIS Instruments.
Loke, M.H., 2011. Encyclopedia of solid earth geophysics. In: Gupta, H.K. (Ed.), Electrical Resistivity Surveys and Data Interpretation. Springer, Netherlands, Dordrecht, pp. 276–283. https://doi.org/10.1007/978-90-481-8702-7_46.
Loke, M.H., Barker, R.D., 1996. Rapid least-squares inversion of apparent resistivity pseudosections by a quasi-Newton method1. Geophys. Prospect. 44, 131–152. https://doi.org/10.1111/j.1365-2478.1996.tb00142.x.
Mohammed, N., 2014. Investigating the behavior of alluvial systems, thanks to the classical, isotopic and emerging tracers : case study of the alluvial aquifer of the Allier River (Auvergne, France). Bordeaux.
Mohammed, N., Celle-Jeanton, H., Huneau, F., Le Coustumer, P., Lavastre, V., Bertrand, G., Charrier, G., Clauzet, L.M., 2014. Isotopic and geochemical identification of main groundwater supply sources to an alluvial aquifer, the Allier River Valley (France). J. Hydrol. 508, 181–196. https://doi.org/10.1016/j.jhydrol.2013.10.051.
Négrel, P., Petelet-Giraud, E., Widory, D., 2004. Strontium isotope geochemistry of alluvial groundwater: a tracer for groundwater resources characterisation. Hydrol. Earth Syst. Sci. 8, 959–972. https://doi.org/10.5194/hess-8-959-2004.
Négrel, Ph., Petelet-Giraud, E., Barbier, J., Gautier, E., 2003. Surface water–groundwater interactions in an alluvial plain: chemical and isotopic systematics. J. Hydrol. 277, 248–267. https://doi.org/10.1016/S0022-1694(03)00125-2.
Ounaïes, S., Schäfer, G., Trémolières, M., 2013. Quantification of vertical water fluxes in the vadose zone using particle-size distribution and pedology-based approaches to model soil heterogeneities. Hydrol. Process. 27, 2306–2324. https://doi.org/10.1002/hyp.9365.
Pastre, J.F., 1986. Altération et paléoaltération des minéraux lourds des alluvions pliocenes et pleistocenes du bassin de l’Allier (Massif central, France). Quaternaire 23, 257–269. https://doi.org/10.3406/quate.1986.1821.
Penna, D., Stenni, B., Sanda, M., Wrede, S., Bogaard, T.A., Gobbi, A., Borga, M., Fischer, M.C., Bonazza, M., Charova, Z., 2010. On the reproducibility and repeatability of laser absorption spectroscopy measurements for ??2H and ??18O isotopic analysis. Hydrol. Earth Syst. Sci. Discuss. 14. https://doi.org/10.5194/hess-14-1551-2010.
Petelet-Giraud, E., Casanova, J., Chery, L., Negrel, P., Bushaert, S., 2005. Essai de caractérisation isotopique (δ18O et δ2H) du signal metéorique actuel à partir des lacs et réservoirs : application au quart sud-ouest de la France. Houille Blanche 57–62. https://doi.org/10.1051/lhb:200502008.
PNMH, 2014. 3rd National Action Plan for Wetlands (2014-2018). Ministère de l’Écologie, du Développement durable et de l’Énergie, La Défense, France.
Ramsar Convention, 1971. Convention on Wetlands of International Importance Especially as Waterfowl Habitat. Ramsar, Iran. United Nations Treaty series No. 14583. As amended by the Paris Protocol, Dec 3, 1982, and Regina Amendments.
Rathore, V.S., Nathawat, M.S., Champatiray, P.K., 2010. Palaeochannel detection and aquifer performance assessment in Mendha River catchment, Western India. J.

Hydrol. 395, 216–225. https://doi.org/10.1016/j.jhydrol.2010.10.026.
Rollet, A.J., Citterio, A., Dufour, S., Lejot, J., Piegay, H., 2005. Expertise hydro-géomorphologique en vue du diagnostic fonctionnel des habitas, de la restauration du transit sédimentaire et des lônes, volet 1, 2, 3 et 4.
Roux, J.-C., 2006. AQUIFERES ET EAUX SOUTERRAINES DE FRANCE-COFFRET 2 TOME. BRGM, Orléans.
Rozanski, K., Froehlich, K., Mook, W.G., 2001. Environmental isotopes in the hydrological cycle: principles and applications. Volume 3: surface water. IHP-V Tech. Doc. Hydrol. 39.
Rudel, A., 1963. Les minéraux lourds des terrasses Quaternaires de Limagne d'Auvergne et leséruptions montdoriennes. Soc Géol Fr Bull 7, 468–469.
Sarris, T.S., Close, M., Abraham, P., 2018. Using solute and heat tracers for aquifer characterization in a strongly heterogeneous alluvial aquifer. J. Hydrol. 558, 55–71. https://doi.org/10.1016/j.jhydrol.2018.01.032.
Sinha, R., Yadav, G.S., Gupta, S., Singh, A., Lahiri, S.K., 2013. Geo-electric resistivity evidence for subsurface palaeochannel systems adjacent to Harappan sites in north-west India. Quat. Int. Geoarchaeol. 308–309, 66–75. https://doi.org/10.1016/j.quaint.2012.08.002. A toolbox of approaches applied in a multidisciplinary research discipline.
Sutton, M.A., Bleeker, A., Howard, C.M., Bekunda, M., Grizzetti, B., de Vries, W., van Grinsven, H.J.M., Abrol, Y.P., Adhya, T.K., Billen, G., Davidson, E.A., Datta, A., Diaz, R., Erisman, J.W., Liu, X.J., Oenema, O., Palm, C., Raghuram, N., Reis, S., Scholz, R.W., Sims, T., Westhoek, H., Zhang, F.S., 2013. Our Nutrient World: The Challenge to Produce More Food and Energy with Less Pollution. NERC/Centre for Ecology & Hydrology, Edinburgh.
Teles, V., Delay, F., de Marsily, G., 2004. Comparison of genesis and geostatistical methods for characterizing the heterogeneity of alluvial media: groundwater flow and transport simulations. J. Hydrol. 294, 103–121. https://doi.org/10.1016/j.jhydrol.2003.11.041. Stochastic Models of Flow and Transport in Multiple-scale Heterogeneous Porous Media.
Tockner, K., Schiemer, F., Baumgartner, C., Kum, G., Weigand, E., Zweimüller, I., Ward, J.V., 1999. The Danube restoration project: species diversity patterns across connectivity gradients in the floodplain system. Regulated Rivers Res. Manage. 15, 245–258. https://doi.org/10.1002/(SICI)1099-1646(199901/06)15:1/3<245::AID-RRR540>3.0.CO;2-G.
UNEP, 2016. A Snapshot of the World's Water Quality: Towards a global assessment. United Nations Environment Programme, Nairobi, Kenya.
Vanderhaeghe, O., Prognon, F., 2012. Saint-Germain-Lembron. Carte géologique de la France à 1 (50), 000.
Veldkamp, E., Jongmans, A.G., 1990. Weathering of alcali basalt gravel in two older Allier river terraces, Limagne, France. Chem. Geol. Geochem. Earth's Surf. Min. Form. 84, 148–149. https://doi.org/10.1016/0009-2541(90)90193-B.
Ward, J.V., Tockner, K., Arscott, D.B., Claret, C., 2002. Riverine landscape diversity. Freshwater Biol. 47, 517–539. https://doi.org/10.1046/j.1365-2427.2002.00893.x.
Winter, T.C., Harvey, J.W., Franke, O.L., Alley, W.M., 1998. Ground water and surface water; a single resource (USGS Numbered Series No. 1139), Circular. U.S. Geological Survey.
Wren, D.G., Davidson, G.R., Walker, W.G., Galicki, S.J., 2008. The evolution of an oxbow lake in the Mississippi alluvial floodplain. J. Soil Water Conserv. 63, 129–135. https://doi.org/10.2489/jswc.63.3.129.
Yang, C., Cai, X., Wang, X., 2018. Remote sensing of hydrological changes in Tian-e-Zhou Oxbow Lake, an Ungauged Area of the Yangtze River Basin. Remote Sens. 10, 1-N.PAG. https://doi.org/10.3390/rs10010027.